Design of castellated steel beams

by

Kyle Bauer

B.S., Kansas State University, 2021

A REPORT

submitted in partial fulfillment of the requirements for the degree

MASTER OF SCIENCE

GE Johnson Department of Architectural Engineering and Construction Science
Carl R. Ice College of Engineering

KANSAS STATE UNIVERSITY
Manhattan, Kansas

2021

Approved by:

Major Professor
Bill Zhang, Ph.D., P.E., S.E.

# Copyright

# Abstract

The goal of this report is to obtain a better understanding of the behavior and design of castellated beams. Castellated steel beams are efficient members for steel gravity systems. Steel I-beams are commonly used in steel building floors, but require large sizes for long spans. A castellated beam is fabricated by cutting W-beams in a certain pattern and welding the parts together to create a deeper section with hexagon openings in the web. Creating a castellated beam from a root I-beam increases strength and stiffness of the member and allows it to support loads at longer spans without increasing beam self-weight. Having a higher moment capacity decreases the number of beams in a bay and lowers both material and connection costs. In addition, the web openings allow integration for MEP systems by running conduits, pipes, and ductwork through the beam.

Due to the web openings, castellated beams behave differently than typical I-beams. Web openings complicate the design and fabrication of castellated beams as they have additional limit states to be checked. American Institute of Steel Construction (AISC) Design Guide 31: *Castellated and Cellular Beam Design* (2016) provides details on how to design castellated beams. The design equations determine both global and local forces acting on castellated beams as well as unique design strength calculations. Other design strengths can be found in AISC 360 *Specification for Steel Buildings*.

This report examines the design procedure of castellated beams and highlights the uniqueness of their design. Two design examples were presented to illustrate the design procedures, one without and one with a composite floor system.

# Table of Contents

# List of Figures

# List of Tables

# List of Notations

$\Delta$ – deflection

$\theta$ – angle theta

$\phi_b$ – resistance factor for bending

$\phi_c$ – resistance factor for compression

$\phi_v$ – resistance factor for shear

A – area

$A_{gross}$ – area of castellated beam through a web segment

$A_{gv}$ – gross area in shear

AISC – American Institute of Steel Construction

$A_{net}$ – net area of castellated beam through a web opening

$A_{nv}$ – net area in shear

$A_{tee}$ – top or bottom tee are of a castellated beam

$A_w$ – area of web

b – horizontal length of hexagon diagonal segments, half of the flange width

$b_f$ – width of flange

$b_{effec}$ – compression width

bot – bottom

$C_{v2}$ – web shear buckling coefficient

$C_w$ – warping constant

d – depth of steel beam

$d_{effec}$ – effect depth of castellated beam

$d_g$ – gross depth of a castellated beam

DG 31 – AISC Design Guide 31 C*astellated and Cellular Beam Design* (AISC, 2016)

DL – dead load

$d_t$ – height of tee section, minimum height of castellated segment

E – modulus of elasticity

e – horizontal length of hexagon edge

Eqn – Equation

$F_{cr}$ – critical stress

$F_e$ – elastic buckling stress

ft - feet

$F_u$ – tensile stress

$F_y$ – yield stress

G – shear modulus

H – flexural constant

h – height difference in the web cut, $h_o/2$

$h_o$ – height of web opening

in - inch

$I_x$ – moment of inertia about the X-axis

$I_{x,gross}$ – moment of inertial for a castellated beam through a web segment

$I_{x,net}$ – moment of inertia for a castellated beam through a web opening

$I_y$ – moment of inertia about the Y-axis

J – polar moment of inertia

k - kips

K – effective length factor

$K_{des}$ – edge of flange to end of fillet distance

klf – kips per linear foot

ksi – kips per square inch

$k_v$ – web plate shear buckling coefficient

K – effective length factor for flexural buckling

L – laterally unbraced length of member

$L_c$ – KL, effective length of member

LL – live load

$M_{cx}$ – available flexural strength along the X-axis

$M_{cy}$ – available flexural strength along the Y-axis

$M_n$ – nominal flexural strength

$M_{ocr}$ – critical moment for web post lateral buckling

$M_p$ – plastic moment

$M_r$ – global moment force

$M_{rx}$ – required flexural strength along the X-axis

$M_{ry}$ – required flexural strength along the Y-axis

$M_{vr}$ – moment due to Vierendeel mechanism

$P_c$ – available axial strength

$P_r$ – axial force on tee section from global moment

psf – pounds per square foot

psi – pounds per square inch

Qn – nominal shear strength of one steel headed stud anchor, kips

$R_n$ – design strength

$\overline{r}_o$ – polar radius of gyration about the shear center

$r_x$ – radius of gyration about X-axis

$r_y$ – radius of gyration about Y-axis

S – spacing of web openings

SPEC – AISC *Specification*

$S_x$ – elastic section modulus about the X-axis

$S_{x,gross}$ – elastic section modulus for a castellated beam through a web segment

$S_{x,net}$ – elastic section modulus for a castellated beam through a web opening

$S_y$ – elastic section modulus about the Y-axis

$t_f$ – thickness of flange

$T_r$ – tensile force

$t_w$ – thickness of web

$V_n$ – shear design strength

$V_r$ – global shear force

$V_{uh}$ – ultimate horizontal shear force

Wu – ultimate linearly distributed load

$x_o$, $y_o$ – coordinates of the shear center with respect to the centroid

$Y_{PNA}$- plastic neutral axis from flange edge

$\overline{y}_{TEE}$ - centroid with respect to the Y-axis

$Z_x$ – plastic section modulus about the X-axis

$Z_{x,gross}$ – elastic section modulus for a castellated beam through a web segment

$Z_{x,net}$ – plastic section modulus for a castellated beam through a web opening

$Z_y$ – plastic section modulus about the Y-axis

# Acknowledgements

Thank you to all of my teachers, professors, and peers who have helped me and been at my side through my education career. I also want to thank Kimberly Kramer and Katie Loughmiller, my committee members, who have helped guided me along my professional career. A big thank you goes also to my parents, who have provided so much for me and helped me grow into who I am today. Lastly a large thank you to my major professor Bill Zhang, who has pushed and encouraged me throughout my years at Kansas State University.

# Chapter 1 – Introduction

Steel beams are a common building element of gravity systems in steel buildings. With standardized shapes and loading tables, I-shaped wide flange (W) beams are easy to design and construct, and are generally used for spans of 20 to 40 feet. For longer spans, W-beams may become inefficient requiring large sizes. Instead of larger W-sections, castellated beams can be used. To make a castellated beam, a W-beam is cut in a jigsaw pattern down the web into two equal pieces. The two pieces are then staggered and reattached by welding, as shown in Figure 1-1. This increases the effective depth of the beam, and thus the moment capacity, while maintaining the same material weight.

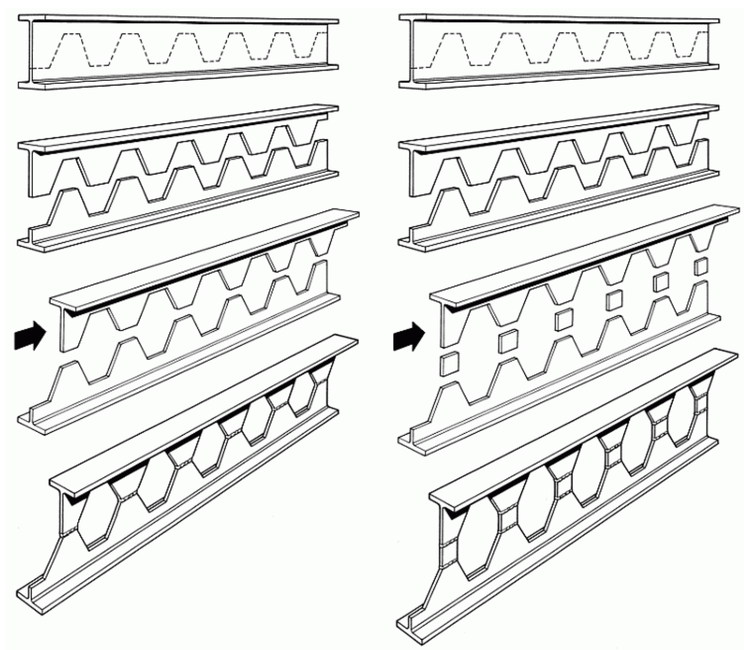

Note: From *What are Castellated Beams?* by J. Grübauer,

(http://www.grunbauer.nl/eng/wat.htm).

**Figure 1-1 – Castellated Beam Assembly**

To further increase the effective depth for moment capacity, steel plates can be added between web posts as shown in Figure 1-1. There are two main patterns to cut the beam to make a deeper section. Beams with hexagonal web openings are known as castellated beams. If the W-beam is cut in circular pattern then the web will have circular openings, as shown in Figure 1-2. They are referred to as cellular beams. Producing cellular beams result in some material waste. Both castellated and cellular beams experience stress redistribution around the openings, but have slightly different behaviors and design equations. This report focuses on castellated beams.

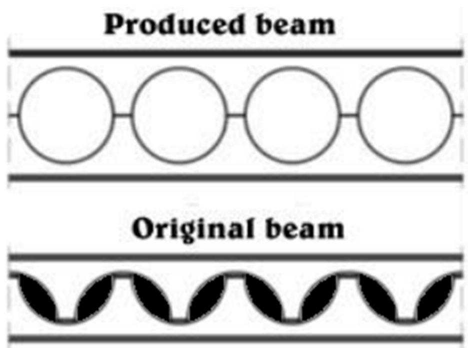


Note: From *Castellated beams* by Marmors Group, (http://www.marmorsgroup.com/steel-structures/castellated-beams).

**Figure 1-2 – Cellular Beam Pattern**

It is possible and sometimes preferable to use two different-sized root beams to produce a castellated section. This is referred to as an asymmetric section, as the top tee and bottom tee sections are different. Asymmetric sections are typically used in composite floors, where the concrete slab resists most of the compression force allowing the top tee to be of a smaller size, while the bottom tee is designed to resist tension and is of a larger size.

One of the benefits of castellated beams is that they have the same connections as typical steel beams. From welded shear tabs to angle seats to double angle bolted or welded connections, all work for castellated beams. Having the same connections as W-beams allows quick installation of connections in the field. Depending on spans and spacings of beams and girders, web openings may be encountered at some connection locations. In such cases, web openings can be filled in full or part with plates, to facilitate the connections.

Other benefits of using castellated beams relate to their effective weight reduction. Using a lighter beam to carry the same load as a heavier beam would reduce beam self-weight and save material. Additionally, deeper sections enable longer spans, commonly up to 60 feet and even 90 feet in some situations. The increased moment capacity of castellated beams will likely reduce the quantity of members of steel framing, and will be more cost effective as more castellated beams are used. While long span W-beam designs are often controlled by deflection requirements, castellated beams have a greater moment of inertia such that deflection will less likely govern the design.

Using castellated beams may reduce floor to floor heights and hence the overall building height by integrating with other systems. Because of web openings, it is possible for electrical, mechanical, and plumbing lines to go through the castellated beams and thus reduce the plenum space required. Penetrating duct sizes are limited to the opening size of the castellated beam. Large ducts will still need to run parallel to castellated beams.

Most engineers are not familiar with castellated beams. With the publication of AISC Design Guide 31: C*astellated and Cellular Beam Design* (AISC, 2016), which is referred to as DG 31, engineers now have a better understanding and necessary tools to design castellated beams.

This report examines the process for designing castellated beams. First, the dimension variables are defined for castellated beams. Changing these dimensions impacts the various design strengths of the beam. This makes castellated beams versatile as they can be efficiently designed on a case by case basis. Next, the limit states to be checked are listed and explained.

Lastly, two examples are worked out going over each of the limit states to illustrate the design process.

# Chapter 2 – Design Patterns of Castellated Beams

Due to the unique geometry, castellated beams behave differently than traditional steel W-beams. Castellated beams will develop local forces necessary to transfer shear and moment around web openings. Web opening dimensions influence the magnitude of these local forces and the stress distribution. Optimizing these dimensions allows beams to be designed more efficiently on a case by case basis than choosing a beam from tables.

## Web Opening Patterns

Many variables influence the design of castellated beams. Because no requirements of opening dimensions exist, there are many cutting patterns for determining the dimensions of the web opening. Among the patterns, the common characteristics include a depth of 1.5 times the base beam depth and an angle of cut close to 60°. Web posts with a 60° cut have a higher flexural capacity than shallower angels. In Europe, the traditional pattern is the Peiner-Schnittührung (Grünbauer). This pattern determines the castellated beam as a series of ratios based on the height of the beam, as shown in Figure 2-1.

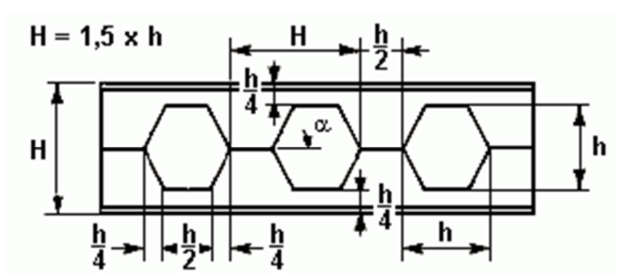


Note: From *Traditional Patterns* by J. Grübauer, (https://www.grunbauer.nl/eng/raatvorm.htm).

**Figure 2-1 – Peiner-Schnittührung Pattern**

By using ratios to determine all the dimensions, it becomes straightforward to create a section property table to facilitate the design for a castellated beam. Examples of these tables can be found on Grübauer BV, where extensive section properties are listed for different beam sizes.

Using those tables greatly helps engineers calculate design capacity of a beam under a given span.

Instead of using a predetermined cutting pattern, a custom cut can also be used. When deciding on the length of cuts, there are three primary variables to decide. The first is the horizontal length of the longitudinal cut, which is defined as *e*. Next is *h*, the vertical offset between the horizontal cuts which determines the web post height. The third is *b*, the horizontal length of the angled cut. These variables are shown in Figure 2-2.

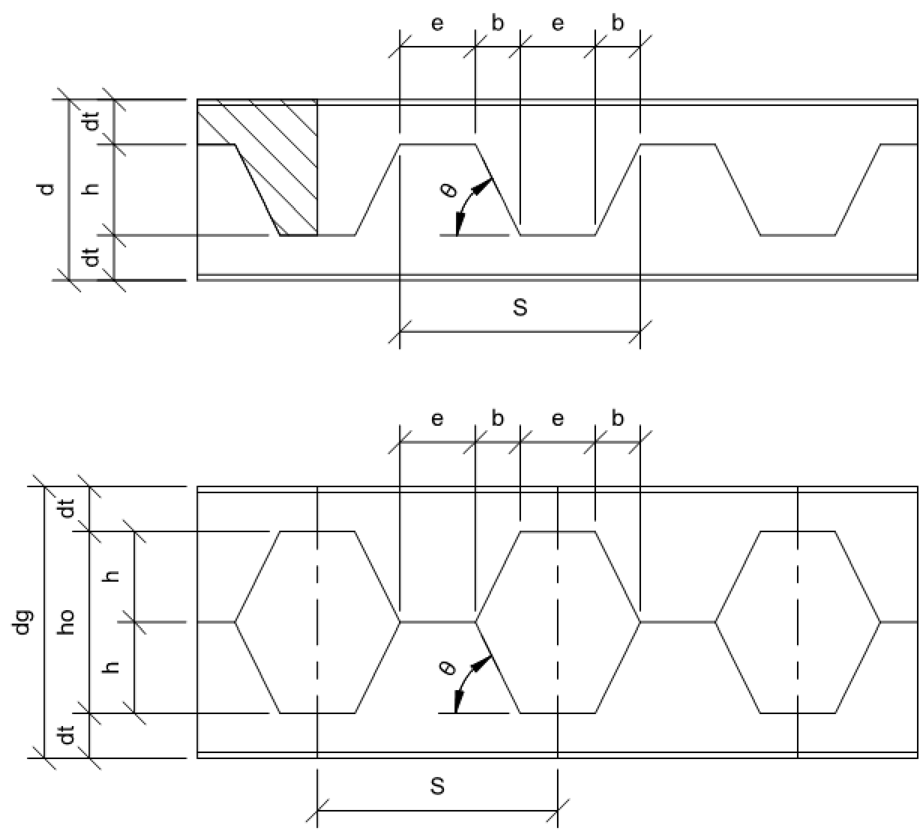


**Figure 2-2 – Castellated Beam Variables**

Once the cutting variables are chosen, the remaining height dimensions can be determined from the base beam selected. These dimensions include $d_t$, depth of the tee section, $d_g$, the gross depth of the castellated beam, and $h_o$, height of the opening, as shown in Figure 2-2.

## Choosing a Base Beam

If castellated beam design tables are not being utilized, a base beam will need to be selected. The required moment of inertia of the beam to meet serviceability is calculated first. The first iteration can start with a section with $I_x$ of half the required moment of inertia value. Beams with the largest $I_x$ per unit mass are found in AISC *Steel Construction Manual* (AISC, 2017) Table 3-3. With a chosen beam, a cutting pattern is then determined along with the properties of the castellated beam. Using these properties, limit states of tee axial strength, tee flexural strength, tee combined forces, web post flexural strength, horizontal shear strength, and vertical shear strength, are checked. If the beam meets all of them, then the beam design is satisfactory. If strength limit state checks indicate a smaller base beam can be used, another iteration is necessary until the lightest section is chosen. Having a spreadsheet or program to check each limit state makes finding a base beam easy.

If a beam fails in one or more limit state checks, there are two options. First, a larger base beam can be used. For a base beam with multiple strength check failures, it is best to upsize. Alternatively, if the beam only fails in one or two limit states, the cutting pattern dimensions could be adjusted. Being able to tweak the dimension variables gives castellated beams more versatility than standard wide flange beams when designing on a case by case basis.

Optimizing a castellated beam design involves both selecting a lightest base beam section and choosing a proper cutting pattern. Multiple iterations of length calculations are often required. So using a design program and/or a spreadsheet is helpful and even necessary. The nomenclature for naming a castellated beam is similar to W-sections with the depth and weight per unit length in the designation. For example, the castellated beam fabricated from a base section W18x40 having a depth of 27 inches would be called a CB27x40. For an asymmetric beam, both base beam weights are listed separated by a slash. If an asymmetric beam was made from a W14x48 for the top tee and a W14x74 for the bottom tee, the castellated beam would be called a CB21x48/74.

## Impacts of Cutting Dimensions

Because the cutting pattern dimensions influence the design strengths, tweaking one or more variables can increase the capacity for a particular limit state. One such variable is *e*, the horizontal length of the cut. This length determines the net width of the full depth web post and the unbraced length of the tee section. By increasing *e*, the unbraced length of the tee section increases. With the increased length, the tee axial strength decreases as it is more prone to buckle. In addition, the Vierendeel moment on the tees also increase with *e*, as a longer section allows more loading and subsequently increases the moment. While the tee section strength decreases, conversely, the web post strengths increase. With a larger web, there is more area for horizontal shear capacity. Furthermore a longer web post has a larger plastic moment which increases the local buckling capacity. The longitudinal cutting length *e* is generally the first variable changed to meet a single limit state.

The next variable is *b*, the horizontal dimension of the angled cut. While *b* does not impact any of the tee strengths, it does influence the web post flexural strength. In conjunction with the vertical dimension of the angled cut, *h*, the angle of the inclined cut is determined. By increasing *b*, the plastic moment of the web post is also increased, but local buckling may govern the flexural strength.

The last variable is *h*, the height of the web post. As it defines the depth of the castellated beam, *h* is rarely changed. Generally, *h* is taken as half the base beam depth so that the castellated beam will have a depth of one and half of the based beam depth. However, castellated beams are not required to be at exactly1.5 the depth of their base beams. By increasing *h*, the effective depth of the beam increases, which increases the section modulus and moment of inertia, moment capacity and stiffness. On the other hand, it reduces the depth of the tee section, $d_t$, and thus the tee area which decreases the axial capacity and flexural capacity of the tee sections. These changes are shown in Figure 2-3. This will have a negative impact of global moment capacity, and may fail the Vierendeel moment check for the tees. To address the failures, *e* should be reduced to increase the axial capacity and decrease the Vierendeel moment. Lastly, increasing *h* increases the web depth, which increases gross section shear capacity.

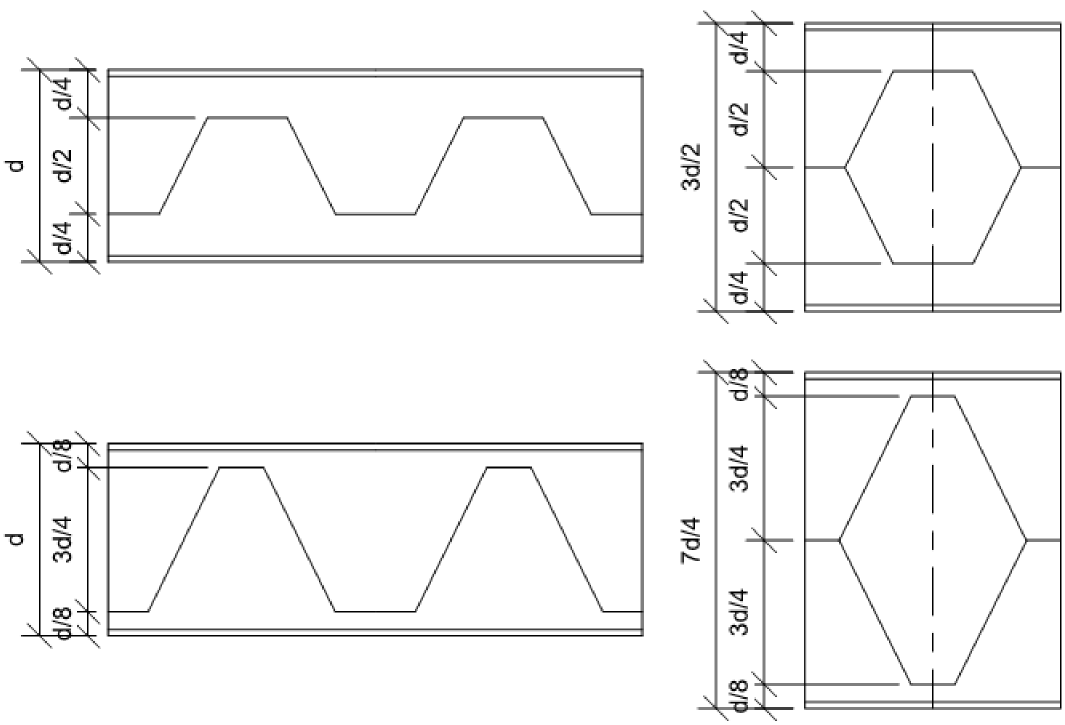


**Figure 2-3 – Comparison of Different *h***

# Chapter 3 – Design Procedure

## Design of Non-composite Castellated Beams

Due to web openings, castellated beams have different design checks compared to solid web W-beams. Castellated beams take the moment similar to a Vierendeel truss. The top and bottom tees will be under compression and tension forces in addition to Vierendeel moments.

Due to web openings, the shear forces cannot be transferred entirely through the web. The tee sections above and below the openings help transfer shear forces along the length of the beam. Shear forces through the tee section creates a moment distribution along the length the tee sections, with the maximum moments at the ends. This is referred to as Vierendeel bending, where plastic hinges may form around the opening. In addition, the tee sections also have to resist axial forces caused by the beam moment, and are thus subject to combined forces checks. If any of these design limit states are not met, a tee section in the castellated beam could fail leading to total beam failure.

Shear checks for a castellated beam are similar to rolled beam shapes. Vertical checks include at the first or last opening where tee sections experience large shear forces but minimum effective areas to resist shear, and at the ends through the gross area where the maximum shear forces occur. In addition, horizontal shear exists through the web posts between the openings. To maintain continuity from axial forces due to global moment, the web post has to withstand the difference between the top and bottom forces. The horizontal shear is checked at the connection between top and bottom tees. Because of that shear force, a moment is created on the web post, which needs to be checked.

The following limit states need to be checked:

1. Tee Axial Strength
2. Tee Flexural Strength
3. Tee Combined Axial and Flexural Forces
4. Web Post Flexural Strength
5. Horizontal Shear Strength
6. Vertical Shear Strength
7. Vertical Shear at Gross Section

After these strength limit states have been checked, the castellated beam is then checked for deflection to meet serviceability.

## Tee Axial Strength

The global moment along the beam length causes compression and tension forces in tee sections, as illustrated in Figure 3-1.

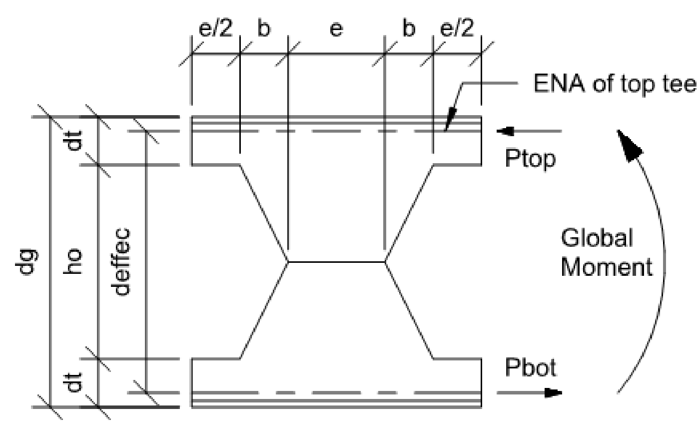


**Figure 3-1 – Axial Forces Derivation**

The sum of the moments from both the tension and compression axial forces at any point must equal the global moment. Since no net axial force on the section occurs, the tension and compression axial forces are equal in magnitude, and can be calculated from the moment and the distance between centroids.

$$P_r = \frac{M_r}{d_{effec}} \qquad \text{(DG 31 Eq'n 3-1)}$$

Where $P_r$ is the required axial tension or compression strength on the tee sections. Typically, compression will govern the design of the tee sections. Axial compression capacity can be governed by flexural buckling or flexural-torsional buckling as stipulated in AISC 360 *Specification for Structural Steel Buildings* (AISC, 2017) Chapter E. The tee section behaves like a column of height $e$, or the length of maximum web opening. Furthermore DG 31 assumes translation and rotation to be fixed in the plane of the web and pinned normal to the web. The end conditions are shown in Figure 3-2. In accordance with Table C-A-7.1 in the AISC *Steel Construction Manual* (AISC, 2017), the effective length factor of the tee is 0.65 for $K_x$ and 1.0 for $K_y$.

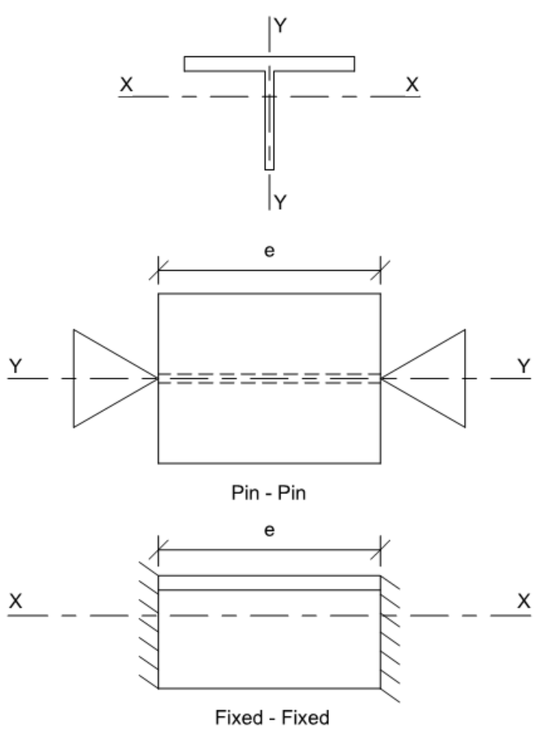


**Figure 3-2 – Tee Section Boundary Conditions**

## Tee Flexural Strength

The global shear force at the locations of web openings is shared by both tee sections. This shear causes fix-end moments in the tee similar to moments in columns of a rigid frame. The moments developed are referred as Vierendeel moments. The moment arm is taken from the mid-span of the tee to where the web starts to join, or *e*/2, as shown in Figure 3-3. For asymmetric castellated beams where two tee sections are of different areas, the shear forces are proportional the tee section areas, so the larger tee will have greater moments developed in it.

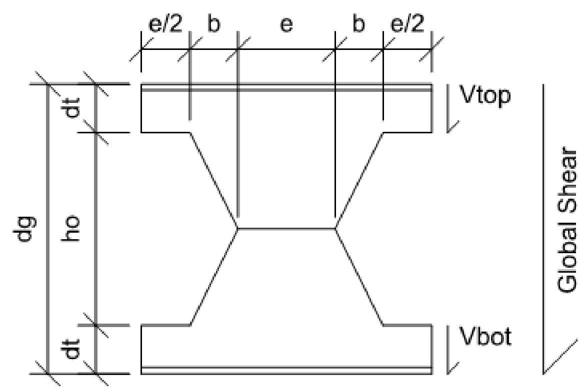


**Figure 3-3 – Vierendeel Moment Derivation**

For castellated beams that have the same tee sections at the top and bottom, the global shear will split evenly between both. Neglecting any shear variance across the span of the tee section, the span can be taken as under constant shear. The shear and moment diagrams for the tee section are shown in Figure 3-4. Therefore the maximum Vierendeel moment is calculated by DG Eqn 3-2.

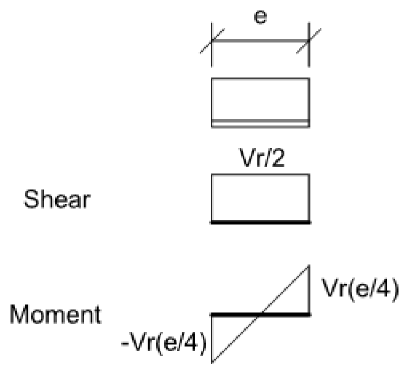


**Figure 3-4 – Vierendeel Forces**

$$M_{vr} = V_r\left(\frac{A_{tee}}{A_{net}}\right)\left(\frac{e}{2}\right) \quad \text{(DG 31 Eqn 3-2)}$$

To resist the Vierendeel moment, the tee section requires adequate flexural strength. The tee flexural strength can be checked in accordance with AISC *Specification* (AISC, 2017) Section F9. Section F9 covers limit states including yielding strength, lateral-torsional buckling, and local buckling of the flange and stem of tees. Because the force is localized to the tee, the unbraced length for lateral-torsional buckling is taken as *e*.

## Combined Forces in Tee Section

With the tee sections under both axial and flexural stresses, each segment needs to be checked for combined forces per AISC *Specification* (AISC, 2017) Chapter H depending on how much of the axial capacity is in use.

When $P_r/P_c$ is greater than 0.2,

$$\frac{P_r}{P_c} + \frac{8}{9}\left(\frac{M_{rx}}{M_{cx}} + \frac{M_{ry}}{M_{cy}}\right) \leq 1.0 \quad \text{(SPEC Eqn H1-1a)}$$

When $P_r/P_c$ is less than 0.2,

$$\frac{P_r}{2P_c} + \left(\frac{M_{rx}}{M_{cx}} + \frac{M_{ry}}{M_{cy}}\right) \leq 1.0 \quad \text{(SPEC Eqn H1-1b)}$$

Because the beam is under a uniform load, the global shear changes at a constant rate. As the Vierendeel moment varies with the global shear for each tee, it will also vary linearly with maximum values towards the beam ends. The axial forces, however, are derived from the global moment which is parabolic for a simple span with maximum at mid-span. With each force having a maximum at different parts of the beam, each tee section along the length will need to be checked as any could be the critical point.

## Web Post Flexural Strength

Similar to how shear through the tee section creates end moments, the web post between openings also experiences a horizontal shear that causing moments. The web post flexural strength may be governed by yielding or local buckling. The horizontal shear through the middle of the web has to balance the difference between the two axial forces in the adjacent top or bottom tees. These forces are shown in Figure 3-4.

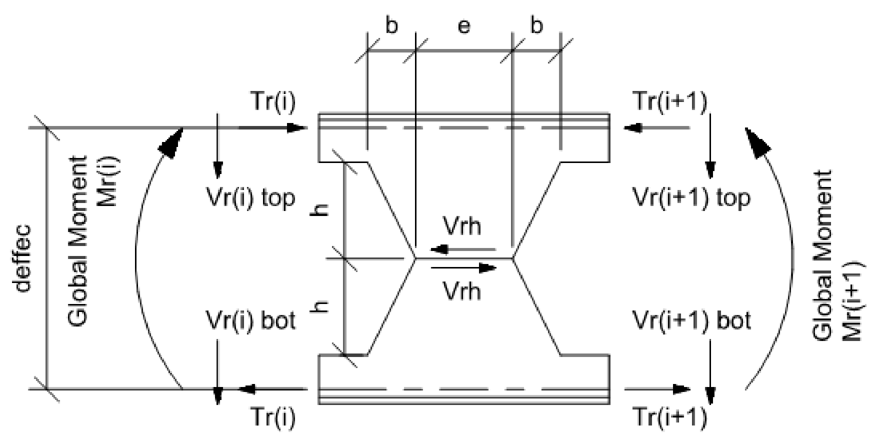


**Figure 3-5 – Web Post Buckling Forces**

Because the axial forces are from the global moment, the horizontal shear can be found from the difference in global moments. As shown in Figure 3-5, at a chosen opening, *i,* and the adjacent opening, *i*+1, for example, the shear on the web post between them can be calculated as:

$$V_{rh} = \left|\frac{M_{r(i+1)} - M_{r(i)}}{d_{effec}}\right| = \left|T_{r(i)} - T_{r(i+1)}\right| \quad \text{(DG 31 Eqn 3-19)}$$

The web post then experiences end moments from the horizontal shear depending on the web post height, $h$. For hybrid sections that use different web heights, both the top and bottom web post will have to be checked.

$$M_{rh} = V_r h \quad \text{(DG 31 Eqn 3-20)}$$

The plastic moment, $M_p$, is calculated assuming the web post section as a rectangle of length $e + 2b$ and thickness of $t_w$ (the root section at the top or bottom of the web post) as shown in DG 31 Equation 3-22. The length $e + 2b$ is used because that is the full length of the connection of the web post to the tee section.

$$M_p = 0.25 t_w (e + 2b)^2 F_y \quad \text{(DG 31 Eqn 3-22)}$$

Because the web post typically has a high $h/t_w$ ratio, flexural strength is governed by local buckling. A reduction factor is then applied to the plastic moment to account for the missing area of the assumed rectangle shape of length $e + 2b$. The reduction factor is a function of $e$, $h$, $t_w$, and the angle $\theta$. DG 31 provides empirical equations for calculating the reduction factor based on experimental studies.

For $\theta = 45°$:

$e/t_w = 10$

$$\frac{M_{ocr}}{M_p} = 0.351 - 0.051\left(\frac{2h}{e}\right) + 0.0026\left(\frac{2h}{e}\right)^2 \leq 0.26 \quad \text{(DG 31 Eqn 3-23)}$$

$e/t_w = 20$

$$\frac{M_{ocr}}{M_p} = 3.276 - 1.208\left(\frac{2h}{e}\right) + 0.154\left(\frac{2h}{e}\right)^2 - 0.0067\left(\frac{2h}{e}\right)^3 \quad \text{(DG 31 Eqn 3-24)}$$

$e/t_w = 30$

$$\frac{M_{ocr}}{M_p} = 0.952 - 0.3\left(\frac{2h}{e}\right) + 0.0319\left(\frac{2h}{e}\right)^2 - 0.0011\left(\frac{2h}{e}\right)^3 \qquad \text{(DG 31 Eqn 3-25)}$$

Values of $e/t_w$ that fall between these equations require interpolation. The maximum value of $M_{ocr}/M_p$ is limited to 0.26, which occurs at $e/t_w = 10$ when $2h/e = 2$.

For $\theta = 60°$:

$e/t_w = 10$

$$\frac{M_{ocr}}{M_p} = 0.587(0.917)^{\frac{2h}{e}} \leq 0.493 \qquad \text{(DG 31 Eqn 3-26)}$$

$e/t_w = 20$

$$\frac{M_{ocr}}{M_p} = 1.96(0.699)^{\frac{2h}{e}} \qquad \text{(DG 31 Eqn 3-27)}$$

$e/t_w = 30$

$$\frac{M_{ocr}}{M_p} = 2.55(0.574)^{\frac{2h}{e}} \qquad \text{(DG 31 Eqn 3-28)}$$

Again for values of $e/t_w$ that fall between the three equations will require interpolation. Compared to $\theta$ of 45°, the 60° equations have a larger cap at $e/t_w = 10$ when $2h/e = 2$ of 0.493 of $M_p$. The reason that the 60° equations have a larger limit is the shape is closer to the assumed rectangle of length $e + 2b$. By looking at extremes, having $\theta$ at 90° is a rectangle of length $e + 2b$ with no need for reduction as no material is missing. Having a small $\theta$ would then mean having a central rectangle with two long triangular shapes on either side to resist the buckling force. Because the triangles are missing most of the web that would resist the force, a higher reduction would have to be applied.

Interpolation for $\theta$ between 45° and 60° is permitted along with using $\phi_b$ for a particular $\theta$. Additionally, the resistance factor varies linearly on the angle between $\phi_b = 0.9$ at 47° to $\phi_b = 0.6$ at 52.5° and back to $\phi_b = 0.9$ at 58° as shown in Figure 3-6.

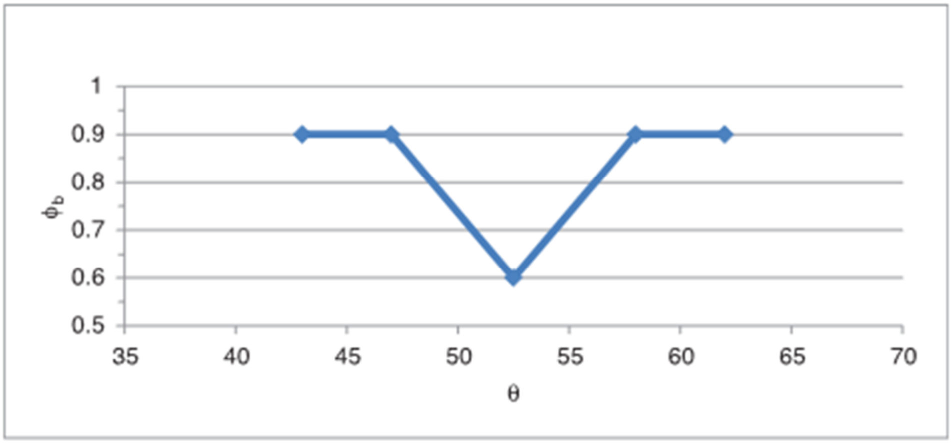


Note: From *AISC Design Guide 31*, 2016, AISC.

**Figure 3-6 – Resistance Factor based on Hexagon Angle**

The design flexural strength of the web post is shown in this section, which is checked against the end moments due to horizontal shear.

$$\phi M_n = \phi_b \left(\frac{M_{ocr}}{M_p}\right) M_p \qquad \text{(DG 31 Eqn 3-29a)}$$

## Horizontal Shear Strength

Castellated steel beam web horizontal shear strength needs to be checked against the horizontal shear force, $V_{rh}$, which was calculated above and was used for the web post flexural strength check. The critical section in the web to resist this shear force is at the joint where the two web posts are welded together. To find the shear strength of the web, AISC *Specification* (AISC, 2017) Section J4.2 can be used. The shear strength of the web at this location is adequate if it's greater than $V_{rh}$,

## Vertical Shear Strength

By looking at the castellated steel beam in vertical segments, two critical locations can be examined for vertical shear. Due to the existence of web openings that reduces web shear strength significantly, the first location is at the net section. The first opening from beam end experiences the largest shear force. The second location is at the beam end. While the shear is maximum at the ends, the gross section can be used with full beam depth. The area of shear for both cases are shown in Figure 3-7. Shear strength check at both of these locations is to follow AISC S*pecification* (AISC, 2017) Chapter G.

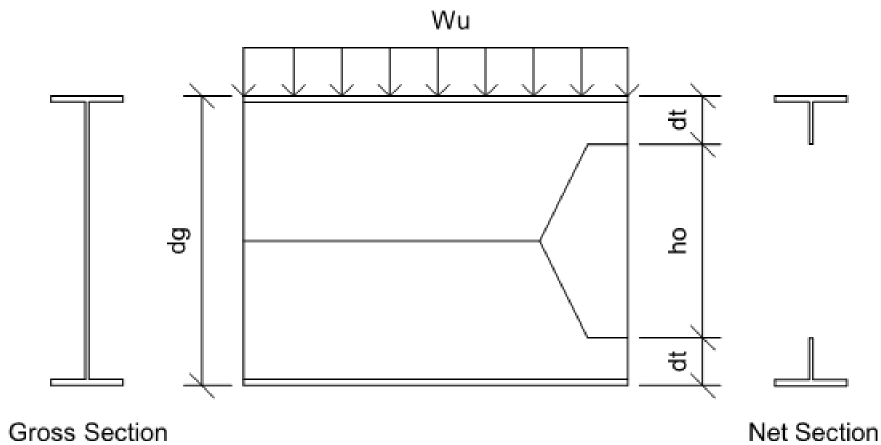


**Figure 3-7 – Vertical Shear Area**

### Deflection

With castellated steel beams having larger depths than typical steel beams, deflection requirements rarely govern castellated beam design. The initial beam chosen to start design to meet deflection requirements would then be the lightest base beam possible. To meet the other limit states which dominate the design, a larger beam has to be used. Previous studies indicated that the beam behave approximately as a prismatic section. However, some shear deformation does occur around openings. To adjust for this, DG 31 approximates deflection calculations by using 90% of the net section moment of inertia for both composite and non-composite members.

## Design of Composite Castellated Beams

Composite castellated beams have the same limit states as non-composite castellated beams. The primary difference comes from the addition of the concrete slab as a compressive element. With the slab taking most of the compression force from the moment, the top beam can be reduced in size as it experiences a smaller compressive force. Another impact from having a concrete slab is that it has a shear capacity. The concrete slab does reduce the shear that causes Vierendeel bending in the tees, and neglecting the shear contribution from concrete slab will be conservative.

First the beam is designed using full composite action. The initial effective depth is determined by DG 31 Eqn 3-8 assuming compression resultant force at the center of topping slab and the tension resultant force at the center of bottom tee. The dimensions used for Eqn 3-8 are shown in Figure 3-8. The effective width, $b_{effec}$, of the concrete slab is the lesser of beam span divided by four and on center spacing of the beams.

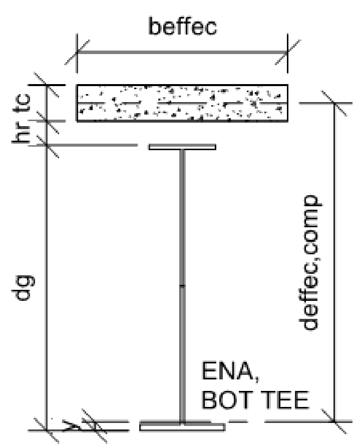


**Figure 3-8 – Effective Composite Depth**

Using the first effective depth, the axial forces are calculated from the global moment as shown in DG 31 Equation 3-9. Then the compression force, which is assumed to be completely in the concrete, is used to find the new depth of the compression block by DG 31 Equation 3-10. The new depth is then used to find the new effective composite depth.

$$d_{effec,comp} = d_g - \overline{y}_{tee,bot} + h_r + 0.5t_c \qquad \text{(DG 31 Eqn 3-8)}$$

$$T_1 = C_1 = \frac{M_r}{d_{effec,comp}} \qquad \text{(DG 31 Eqn 3-9)}$$

$$X_c = \frac{C_1}{0.85 f_c' b_{effec}} \quad \text{(DG 31 Eqn 3-10)}$$

The new compression depth, $X_c$, is then used as $t_c$ in DG 31 Eqn 3-8 to find the new effective depth.

$$d_{effec,comp} = d_g - \overline{y}_{tee,bot} + h_r - \frac{X_c}{2}$$

With a new effective composite depth, a new compression force is found and thus a new compression depth. This cycle continues until the effective composite depth converges. After the depth converges, the updated tension and compression forces are used.

Next the shear capacity of the concrete slab is found by DG 31 Eqn 3-14 and 3-15. This concrete slab shear strength will be used in the calculation of shear in steel.

$$V_{nc} = 3(h_r + t_c)(t_c)4\sqrt{f_c'} \quad \text{(DG 31 Eqn 3-14)}$$

$$V_c = \phi_{cv} V_{nc} \quad \text{(DG 31 Eqn 3-15a)}$$

## Tee Axial Strength

To ensure full composite action, sufficient shear studs are required. AISC *Specification* (AISC, 2017) Section I3.2d provides the equations for determining the nominal shear strength of shear studs. The number of studs required is determined by stud capacity found in AISC *Specification* (AISC, 2017) Section I8. With the specified number of studs, the average stud density, q, is found and relates to how much axial compression of concrete can be developed. At each opening at a distance from the end, the axial compressive force that can be developed in the concrete corresponding to the amount of the studs from the beam end to the opening is compared to the tension force that can be developed in steel. If the concrete compressive is larger, there is full composite action and no compression force in the top tee. If the tension force is larger, the top tee has to make up for the deficiency of compression by using DG 31 Eqn 3-12. These forces are shown in Figure 3-9.

$$T_o = M_r \left[ \frac{1 - \frac{q(X_i)}{T_{1(i+n)}}}{d_{effec}} \right] \qquad \text{(DG 31 Eqn 3-12)}$$

Typical initial design assumes the beam has sufficient number of studs to achieve full composite action. By designing for full composite action, the top beam is designed around the tee flexural strength instead of compression and combined forces. Removing the compression force from the top beam allows a lighter beam section to be used. In addition the bottom beam section is designed around the tension force instead of compression which would otherwise have a smaller capacity. If too many studs are required for full composite action, then partial action could be investigated in subsequent design iterations. Partial action would mean the top tee sections would experience a compression force from DG 31 Eqn 3-12 and would need to be checked according to AISC *Specification* (AISC, 2017) Chapter E.

The tensile capacity is then determined in accordance with AISC *Specification* (AISC, 2017) Section D2. If the beam does not have full composite action, then the top tee will have a compression force. The compression capacity of the top tee is then found in accordance with AISC *Specification* (AISC, 2017) Chapter E.

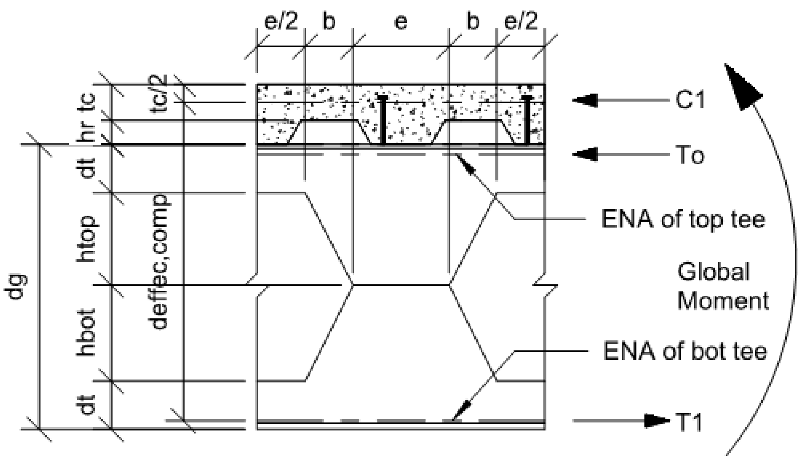


**Figure 3-9 – Composite Axial Forces**

## Tee Flexural Strength

The Vierendeel bending moments are determined from the net shear the tee sections experience. The net shear experienced by the steel is the global shear minus the shear strength from concrete slab, as in DG 31 Eqn 3-16.

$$V_{net} = V_r - V_c \qquad \text{(DG 31 Eqn 3-16)}$$

The net shear is then shared by two tees proportional to their areas, so for a composite beam that utilizes an asymmetric beam, the larger tee will have a larger Vierendeel moment. The Vierendeel moment is calculated by DG 31 Eqn 3-17. Shear forces used to calculate the Vierendeel moment are shown in Figure 3-10.

$$M_{vr} = V_{net}\left(\frac{A_{tee}}{A_{net}}\right)\left(\frac{e}{2}\right) \qquad \text{(DG 31 Eqn 3-17)}$$

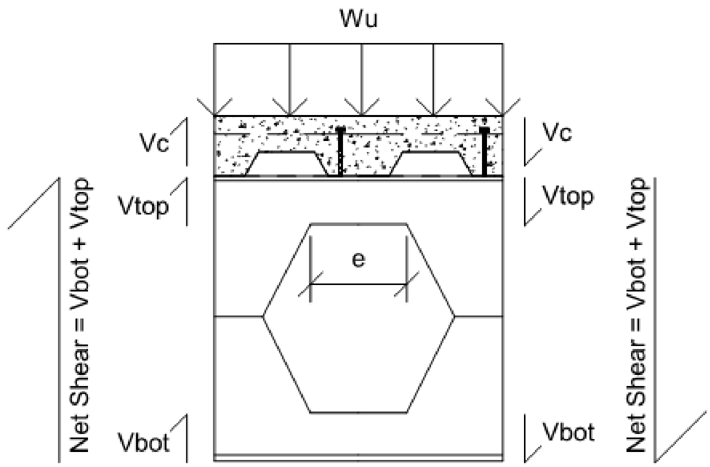


**Figure 3-10 – Composite Vierendeel Moment Derivation**

The flexural capacity of the tee section is determined the same way as in non-composite design by AISC *Specification* (AISC, 2017) Section F9. Limit states include yielding under the assumption that tee stem is in tension. Lateral-torsional buckling is also checked with the assumption of the stem being in compression. The length, $L_b$, is taken as the length of the tee section, *e*. Flange local buckling is checked if flanges are not compact. Lastly local buckling of tee stem is checked and the flexural capacity is the smallest of these four limit states.

## Combined Forces

The bottom tee does experience both flexural and axial forces, and will need to be check with combined forces. The top tee is only checked for combined forces if there is partial composite action. Otherwise, there is no compression force in the top tee. The concrete slab resists a portion of total shear, so the net shear is used for combined forces. Because of this, at midspan there may not be any shear experienced by the tees. Combined forces are checked by AISC *Specification* (AISC, 2017) Section H1.1.

## Web Post Flexural Strength

Web post flexural strength is determined in the same way as the non-composite beam. The moment is determined by taking the hole heights as a moment arm for the horizontal shear, as shown in Figure 3-11. The difference for composite beams compared to non-composite beams is that top and bottom tees will have different moments based on the different heights and they also have different moment strengths. The strength equations for both tees are the same set of equations for a non-composite beam.

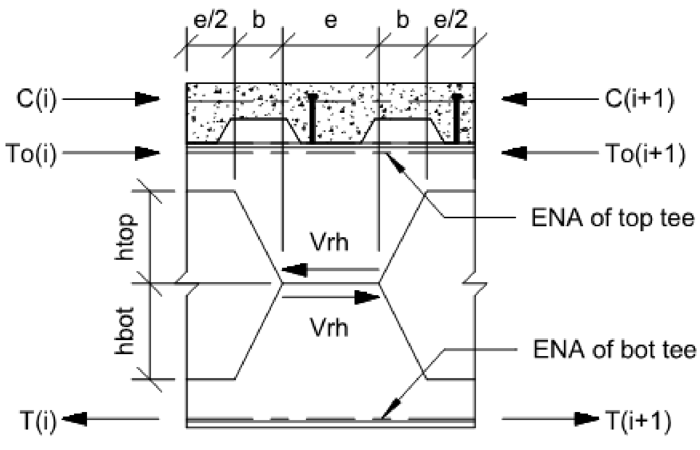


**Figure 3-11 – Composite Web Post Buckling Terms**

## Horizontal Shear

Using DG 31 Eqn 3-19, the horizontal shear can be found by taking the difference in tension forces from adjacent openings. These forces are shown in Figure 3-11.

$$V_{rh} = \left|\frac{M_{r(i+1)} - M_{r(i)}}{d_{effec}}\right| = \left|T_{r(i)} - T_{r(i+1)}\right| \qquad \text{(DG 31 Eqn 3-19)}$$

The critical location for horizontal shear is where two webs are connected. As the top and bottom have different thicknesses, the smaller of the two is used to determine capacity according to AISC Specification (AISC, 2017) Chapter J.

## Vertical Shear

For vertical shear checks, the global shear force is used conservatively. At the net section, the shear is again proportioned to either tee based on their areas in the same way as finding the Vierendeel bending moment. The shear capacity of each tee is then determined in accordance with AISC S*pecification* (AISC, 2017) Section G3.

At the gross section, AISC *Specification* (AISC, 2017) G2 is used. Again with different web thicknesses at the top and bottom, the smaller one is used along the entire beam height.

## Deflection

Before composite action develops, the net moment of inertia of steel only is used with the dead load of the beam and slab. Afterwards the composite moment of inertia can be used for live load and superimposed dead load deflection checks. As in the non-composite deflection checks, only 90% of moment of inertia can be used.

# Chapter 4 – Design Examples

## General Design Parameters

Two design examples are presented in this chapter. Both are based on a 40 foot by 40 foot typical bay in an office building. 40 feet was chosen as it is the smallest span that castellated beams can start to be more efficient than W-beams. From the ASCE 7-16 (ASCE, 2017) Table 4.3-1 a live load of 50 psf is used. No partition loads are included as the purpose of the examples are to work through the design equations and check limit states, not design for this exact office bay.

## Non-composite Beam Design

The non-composite floor system consists of 66-S six-inch precast hollowcore normal weight concrete planks with a two inch topping for a total weight of 74 psf (PCI 2017). This was chosen to support the live load over a 20 foot span. The self-weight of the beam is assumed to be less than 100 plf, which becomes five psf spreading out over 20 feet of spacing. No additional structural loads were considered for the design example.

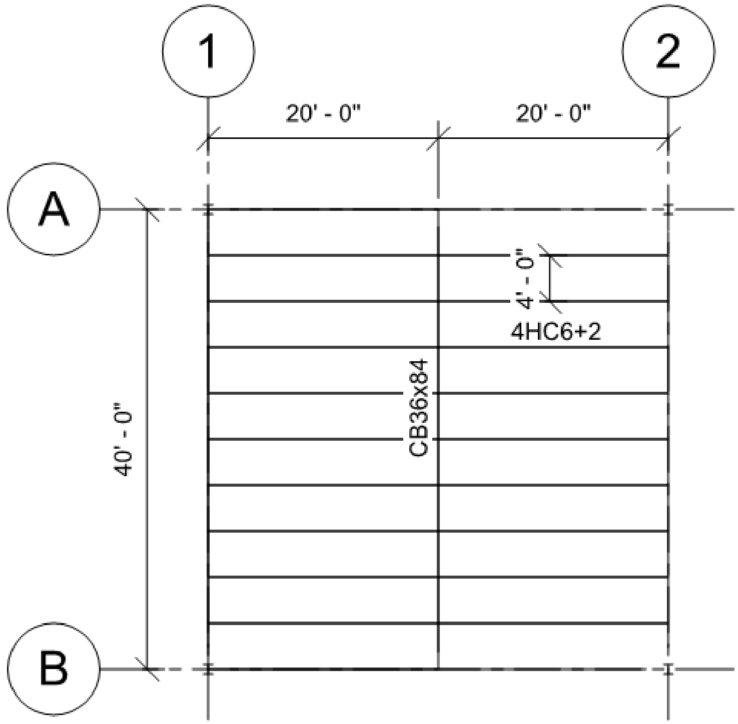


**Figure 4-1 – Bay Floor Plan**

## Base Section Properties

The first step in the design process is to determine the distributed load on the beam.

$$W_u = 1.2D + 1.6L \qquad \text{(ASCE 7-16 2.3.1.2)}$$

$$W_u = (1.2(74\ \text{psf} + 5\ \text{psf}) + 1.6(50\ \text{psf}))(20\ \text{ft spacing}) = 3.5\ \text{klf}$$

Next, a base beam can be selected. Initial design looked at a W24x84. If a chosen beam failed, the castellated opening dimensions could be changed or the beam could be upsized.

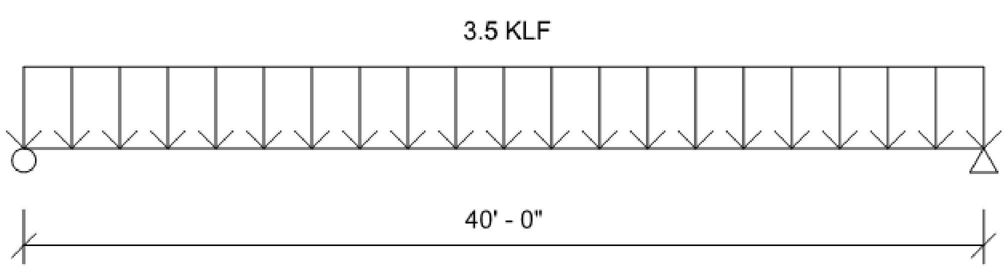


**Figure 4-2 – Beam Loading**

**Table 4-1 – Root Beam Properties**

| Beam | $A$ | $d$ | $t_w$ | $b_f$ | $t_f$ | $k_{des}$ | $I_x$ | $S_x$ | $Z_x$ |
|---|---|---|---|---|---|---|---|---|---|
| W24x84 | 24.7 | 24.1 | 0.470 | 9.02 | 0.770 | 1.27 | 2370 | 196 | 224 |

With the base beam dimensions known the castellated beam dimensions can be determined. This design first tried the Peiner-Schnittührung pattern (Grünbauer), presented in Chapter 2. The main properties include a new height ratio of 1.5 and a hexagonal angle of 63.4°. However, using the Peiner-Schnittührung pattern did not meet the limit state of combined forces on the tee section. Instead of choosing a larger base beam, the castellated beam dimensions were modified by decreasing *e* from 12 in. to 10 in., reducing the Vierendeel moment experienced and increasing the axial capacity. The properties for the CB36x84 are listed Table 4-2. Because Vierendeel moments are largest near beam ends, the outermost openings will be infilled. Web openings will begin on the second opening from the cutting pattern as shown in Figure 4-6. Figure 4-3 shows the sections of the original and castellated beams and Figure 4-4 shows the cut and weld pattern for the fabrication of the beam.

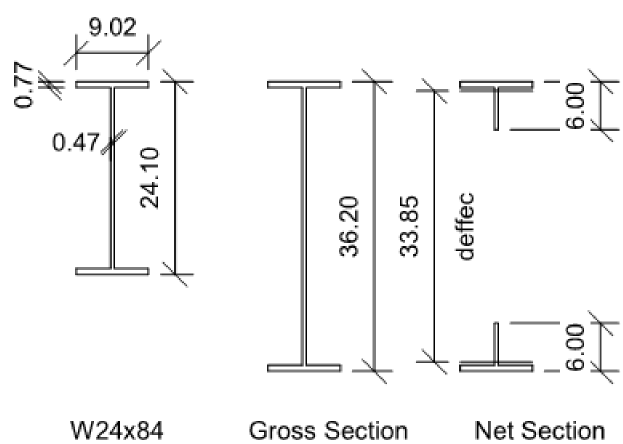


**Figure 4-3 – Beam Section Dimensions**

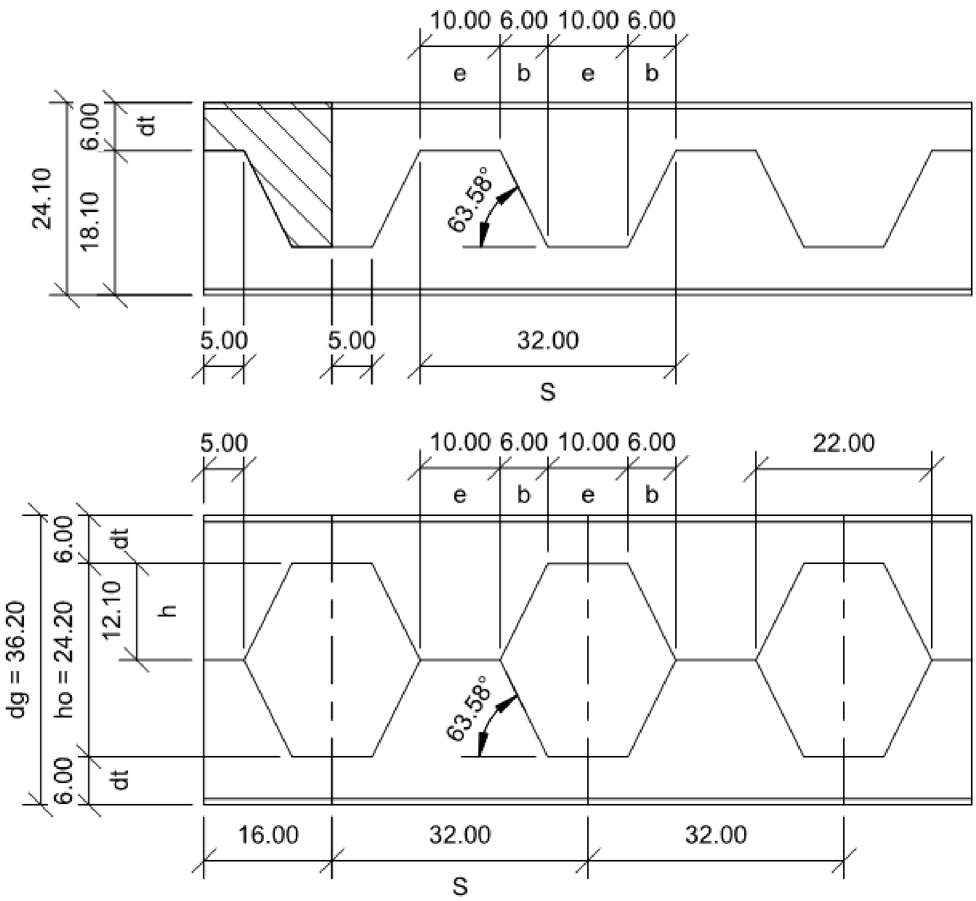


**Figure 4-4 – Castellated Beam Dimensions**

**Table 4-2 – Castellated Beam Dimensions**

| | |
|---|---|
| $d_g = 1.5d =$ | 36.2 in |
| $e =$ | 10 in |
| $b = d/4 =$ | 6.0 in |
| $d_t = d/4 =$ | 6.0 in |
| $h = d - 2d_t =$ | 12.1 in |
| $h_o = d =$ | 24.2 in |
| $S = 2(e+b) =$ | 32 in |
| $\theta = \tan^{-1}(h/b) =$ | 63.6° |

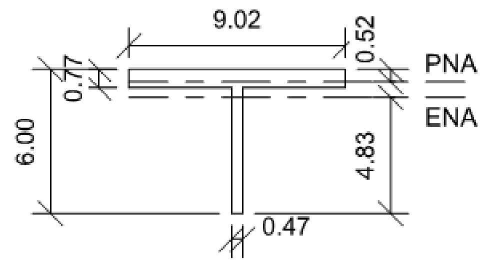


**Figure 4-5 – Tee Section Dimensions**

**Table 4-3 – Tee Section Properties**

| $A$ | $\bar{y}_{TEE}$ | $I_x$ | $I_y$ | $S_x$ | $S_y$ | $Z_x$ | $Z_y$ | $R_x$ | $R_y$ | $Y_{PNA}$ | $J$ | $y_o$ |
|---|---|---|---|---|---|---|---|---|---|---|---|---|
| 9.4 in$^2$ | 4.83 | 22.3 | 47.1 | 4.61 | 10.5 | 8.54 | 16.0 | 1.54 | 2.24 | 0.52 | 1.55 | 4.45 |

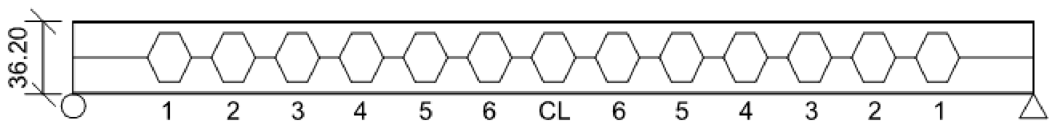


**Figure 4-6 – Castellated Beam Openings**

**Table 4-4 – Web Opening Locations**

| Opening | 1 | 2 | 3 | 4 | 5 | 6 | CL |
|---|---|---|---|---|---|---|---|
| $x$, ft | 4.0 | 6.67 | 9.33 | 12.0 | 14.67 | 17.33 | 20.0 |

First, the section properties of both net section at openings, and gross section between openings, are calculated.

Net section properties

$$A_{net} = 2A_{Tee}$$

$$A_{net} = 2(9.4 \text{ in}^2) = 18.8 \text{ in}^2$$

$$y = \bar{x} = \frac{d_g}{2}$$

$$y = \frac{36.2 \text{ in}}{2} = 18.1 \text{ in}$$

$$d_{effec} = d_g - 2(d_t - \bar{y}_{TEE})$$

$$d_{effec} = 36.2 \text{ in} - 2(6.0 \text{ in} - 4.83 \text{ in}) = 33.9 \text{ in}$$

$$I_{x,net} = 2I_{x,tee} + 2A_{tee}\left(\frac{d_{effec}}{2}\right)^2$$

$$I_{x,net} = 2(22.3 \text{ in}^4) + 2(9.4 \text{ in}^2)\left(\frac{33.9 \text{ in}}{2}\right)^2 = 5446 \text{ in}^4$$

$$S_{x,net} = \frac{I_{x,net}}{\left(\frac{d_g}{2}\right)}$$

$$S_{x,net} = \frac{5446 \text{ in}^4}{\left(\frac{36.2 \text{ in}}{2}\right)} = 300.9 \text{ in}^3$$

$$Z_{x,net} = 2A_{tee}\left(\frac{d_{effec}}{2}\right)$$

$$Z_{x,net} = 2(9.4 \text{ in}^2)\left(\frac{33.9 \text{ in}}{2}\right) = 318.7 \text{ in}^3$$

Gross Section Properties

$$A_{gross} = A_{net} + h_o t_w$$

$$A_{gross} = 18.8 \text{ in}^2 + (24.2 \text{ in})(0.47 \text{ in}) = 30.2 \text{ in}^2$$

$$I_{x,gross} = I_{x,net} + \left(\frac{t_w {h_o}^3}{12}\right)$$

$$I_{x,gross} = 5446 \text{ in}^4 + \left(\frac{(0.47 \text{ in})(24.2 \text{ in})^3}{12}\right) = 6001 \text{ in}^4$$

$$S_{x,gross} = \frac{I_{x,gross}}{\left(\frac{d_g}{2}\right)}$$

$$S_{x,gross} = \frac{6001 \text{ in}^4}{\left(\frac{36.2 \text{ in}}{2}\right)} = 331.5 \text{ in}^3$$

$$Z_{x,gross} = Z_{x,net} + 2t_w h\left(\frac{h}{2}\right)$$

$$Z_{x,gross} = 318.7 \text{ in}^3 + 2(0.47 \text{ in})(12.1 \text{ in})\left(\frac{12.1 \text{ in}}{2}\right) = 387.5 \text{ in}^3$$

Using the distributed load of 3.5 klf, the global shear and moment are found at each point. Next the local beam forces are created from the global forces at the center of each opening. At each section, the local Vierendeel forces can be calculated per DG 31 Eqn 3-1 and 3-2. The local Vierendeel and local axial loads are listed in Table 4-5.

$$P_r = \frac{M_r}{d_{effec}} \qquad \text{(DG 31 Eqn 3-1)}$$

$$P_r = \frac{M_r}{33.9 \text{ in}}$$

$$M_{vr} = V_r\left(\frac{A_{tee}}{A_{net}}\right)\left(\frac{e}{2}\right) \qquad \text{(DG 31 Eqn 3-2)}$$

$$M_{vr} = V_r\left(\frac{9.4 \text{ in}^2}{18.8 \text{ in}^2}\right)\left(\frac{10 \text{ in}}{2}\right)$$

**Table 4-5 – Beam Forces**

| Opening | $x$, ft | $V_r$, k | $M_r$, k-ft | $P_r$, k | $M_{vr}$, k-ft |
|---|---|---|---|---|---|
| Beam CL | 20.0 | 0.0 | 699.2 | 247.8 | 0.0 |
| 6 | 17.3 | 9.3 | 686.8 | 243.4 | 23.3 |
| 5 | 14.7 | 18.6 | 649.5 | 230.2 | 46.6 |
| 4 | 12.0 | 28.0 | 587.3 | 208.1 | 69.9 |
| 3 | 9.33 | 37.3 | 500.3 | 177.3 | 93.2 |
| 2 | 6.67 | 46.6 | 388.4 | 137.7 | 116.5 |
| 1 | 4.0 | 56.0 | 251.7 | 89.2 | 139.8 |
| Beam End | 0 | 70.0 | 0 | 0 | 0 |

With beam forces now known, each limit state can be investigated to determine beam adequacy.

## Tee Axial Strength

Tee Flexural Buckling

In order to determine the axial capacity of the tee section, the flange and web compactness needs to be checked. Case 1 from AISC *Specification* (AISC, 2017) Table B4.1b is used to check if the flanges are slender.

$$\lambda_r = 0.56\sqrt{\frac{E}{F_y}} = 0.56\sqrt{\frac{29{,}000 \text{ ksi}}{50 \text{ ksi}}} = 13.49$$

Width-to-thickness ratio

$$\frac{b}{t} = \frac{b_f}{2t_f} = \frac{9.02 \text{ in}}{2(0.77 \text{ in})} = 5.86$$

Comparing the ratio to the limiting ratio, the flanges are nonslender. Next the tee stems are checked for slenderness under Case 4.

$$\lambda_r = 0.75\sqrt{\frac{E}{F_y}} = 0.75\sqrt{\frac{29{,}000 \text{ ksi}}{50 \text{ ksi}}} = 18.06$$

Width-to-thickness ratio

$$\frac{d}{t} = \frac{d_t}{t_w} = \frac{6.0 \text{ in}}{0.47 \text{ in}} = 12.8$$

Comparing the ratio to the limiting ratio, the tee stem is nonslender. With the tee section having no slender elements, AISC *Specifications* (AISC, 2017) Sections E3 and E4 are used instead of Section E7 for determining axial capacity.

Starting with Section E3, the governing $L_c/r$ ratio is established. As per DG 31, $K_x$ is taken as 0.65 and $K_y$ as 1.0 with the larger of the two ratios governing.

$$\frac{L_c}{r_x} = \frac{K_x e}{r_x} = \frac{0.65(10\text{ in})}{1.54\text{ in}} = 4.22$$

$$\frac{L_c}{r_y} = \frac{K_y e}{r_y} = \frac{1.0(10\text{ in})}{2.24\text{ in}} = 4.46$$

The elastic buckling stress is determined according to AISC *Specification* (AISC, 2017) Eqn E3-4.

$$F_e = \frac{\pi^2 E}{\left(\frac{L_c}{r}\right)^2} \qquad \text{(SPEC Eqn E3-4)}$$

$$F_e = \frac{\pi^2\ 29{,}000\text{ ksi}}{(4.46)^2} = 14{,}389\text{ ksi}$$

Tee Flexural-Torsional Buckling

The second failure method from axial compression is torsional buckling of the tee section. The design strength requirements are outlined in Section E4. Because the tee section is singly symmetric, the elastic stress is determined by AISC *Specification* (AISC, 2017) Eqn E4-3.

$$F_e = \frac{F_{ey} + F_{ez}}{2H}\left(1 - \sqrt{1 - \frac{4F_{ey}F_{ez}H}{\left(F_{ey} - F_{ez}\right)^2}}\right) \qquad \text{(SPEC Eqn E4-3)}$$

$$F_{ey} = \frac{\pi^2 E}{\left(\frac{L_{cy}}{r_y}\right)^2} \qquad \text{(SPEC Eqn E4-6)}$$

$$F_{ez} = \left(\frac{\pi^2 E C_w}{{L_{cz}}^2} + GJ\right)\frac{1}{A_{tee}\bar{r}_o^2} \qquad \text{(SPEC Eqn E4-7)}$$

$$H = 1 - \frac{x_0^2 + y_0^2}{\bar{r}_o^2} \qquad \text{(SPEC Eqn E4-8)}$$

$$\bar{r}_o{}^2 = x_o^2 + y_o^2 + \frac{I_x + I_y}{A_{tee}} \qquad \text{(SPEC Eqn E4-9)}$$

Using the tee section properties, the polar radius of gyration, $\bar{r}_o$, can be found.

$$\bar{r}_o^{\,2} = 0^2 + (4.45\text{ in})^2 + \frac{22.3\text{ in}^4 + 47.1\text{ in}^4}{9.4\text{ in}^2} = 27.19\text{ in}^2$$

The polar radius is then used to find the flexural constant, *H*.

$$H = 1 - \frac{0^2 + (4.83\text{ in})^2}{27.19\text{ in}^2} = 0.142$$

Next the elastic stresses are found. AISC Spec notes that for tee sections, the $C_w$ term is omitted when finding $F_{ez}$. As the portion that can experience flexural-torsional buckling is the tee section, the unbraced length of $L_z$ is taken as e from the castellated steel beam properties.

$$F_{ey} = \frac{\pi^2\ 29{,}000\text{ ksi}}{(4.46)^2} = 14{,}389\text{ ksi}$$

$$F_{ez} = \left(\frac{\pi^2\ 29{,}000\text{ ksi}\ C_w}{(10\text{ in})^2} + (11{,}200\text{ ksi})(1.55\text{ in}^4)\right)\frac{1}{(9.4\text{ in}^2)(27.19\text{ in}^2)} = 79.12\text{ ksi}$$

Now the elastic buckling stress $F_e$ can be found.

$$F_e = \frac{14389\text{ ksi} + 79.12\text{ ksi}}{2(0.142)}\left(1 - \sqrt{1 - \frac{4(14389\text{ ksi})(79.12\text{ ksi})(0.142)}{(14389\text{ ksi} - 79.12\text{ ksi})^2}}\right)$$

$$\mathrm{F_e} = 80.5\text{ ksi}$$

The critical stress $F_{cr}$ is found by using the smaller of the two elastic buckling stresses $F_e$. Here, $F_e$ will be taken as 47.43 ksi from flexural-torsional buckling.

To find the critical stress, Eqn E3-2 or E3-3 is used depending on $F_y/F_e$.

$$\frac{F_y}{F_e} = \frac{50\text{ ksi}}{80.5\text{ ksi}} = 0.621$$

Because $F_y/F_e$ is less than 2.25, AISC Spec Eqn E3-2 is used.

$$F_{cr} = \left(0.658^{\frac{F_y}{F_e}}\right)F_y$$

$$F_{cr} = (0.658^{0.621})50\text{ ksi} = 38.56\text{ ksi}$$

The critical stress is then applied to the tee area to find the axial strength per Eqn E3-1.

$$P_n = F_{cr}A_{tee}$$

$$P_n = (38.56 \text{ ksi})(9.4 \text{ in}^2) = 362.5 \text{ k}$$

Lastly the resistance factor is applied per AISC Spec E1.

$$\phi_c P_n = 0.9(362.5 \text{ k}) = 326.3 \text{ k}$$

Comparing the design capacity to the axial forces from Table 4-5, the maximum axial force the tee section experiences is 248 k at midspan. As this is less than the design capacity, the tee section has adequate axial capacity.

## Tee Flexural Strength

Tee Flexural Yielding

Due to the Vierendeel mechanism from the global shear, the tee sections experience additional stresses from the Vierendeel moment. AISC *Specification* (AISC, 2017) Section F9 outlines the moment capacity of tee sections. The first limit case is yielding, per Eqn F9-1.

$$M_n = M_p \qquad \text{(SPEC Eqn F9-1)}$$

With the tee stems under compressions forces, Eqn F9-4 is used

$$M_p = M_y \qquad \text{(SPEC Eqn F9-4)}$$

$$M_y = F_y S_x \qquad \text{(SPEC Eqn F9-3)}$$

$$M_y = (50 \text{ ksi})(4.61 \text{ in}^3) = 230.5 \text{ k} - \text{in}$$

The nominal moment, $M_n$, for yielding is therefore 230.5 k-in.

Lateral-Torsional Buckling

The unbraced length, taken as e, is compared to the limiting laterally unbraced length, $L_b$.

$$L_b = 1.76 r_y \sqrt{\frac{E}{F_y}} \qquad \text{(SPEC Eqn F9-8)}$$

$$L_b = 1.76(2.24\text{ in})\sqrt{\frac{29{,}000\text{ ksi}}{50\text{ ksi}}} = 94.9\text{ in}$$

Comparing e of 10 in to $L_b$, the limit state of lateral-torsional buckling does not apply.

Flange Local Buckling

Flange compact limits are given in Table B4.1b, Case 10 for tee flanges.

$$\lambda_p = 0.38\sqrt{\frac{E}{F_y}} = 0.38\sqrt{\frac{29{,}000\text{ ksi}}{50\text{ ksi}}} = 9.1516 \qquad \text{(SPEC Eqn F9-8)}$$

Width-to-thickness ratio

$$\frac{b}{t} = \frac{b_f}{2t_f} = \frac{9.02\text{ in}}{2(0.77\text{ in})} = 5.86$$

As the ratio is under the compact limit, the flanges are compact and flange local buckling does not apply.

Tee Stem Local Buckling

Eqn F9-16 limits the strength due to tee stem local buckling.

$$M_n = F_{cr}S_x \qquad \text{(SPEC Eqn F9-16)}$$

The critical force depends on the depth to thickness ratio.

$$\frac{d}{t_w} = \frac{d_t}{t_w} = \frac{6.0\text{ in}}{0.47\text{ in}} = 12.77$$

$$0.84\sqrt{\frac{E}{F_y}} = 0.84\sqrt{\frac{29{,}000\text{ kis}}{50\text{ ksi}}} = 20.23$$

As the length to thickness ratio is less than the first threshold, Eqn F9-17 determines the value of the critical stress.

$$F_{cr} = F_y \qquad \text{(SPEC Eqn F9-17)}$$

$$F_{cr} = 50\text{ ksi}$$

$$M_n = (50\ \text{ksi})(4.61\ \text{in}^3) = 230.5\ \text{k} - \text{in}$$

From the four limit states for tee flexural strength, the smallest nominal moment is used to find the capacity. $M_n$ will be taken as 230.5 k-in from flexural yielding and tee stem local buckling. Substituting into Eqn F9-1 and applying the resistance factor gives the tee flexural capacity.

$$\phi_b M_n = 0.9(230.5\ \text{k} - \text{in}) = 207.5\ \text{k} - \text{in}$$

From Table 4-5, the maximum Vierendeel moment experienced is 140 k-in. No value is listed at the beam end because there is no tee section from an opening there. As the flexural design strength is greater than the Vierendeel moment, the tee section has adequate flexural capacity.

## Combined Forces

With both axial and flexural forces acting on the tee section, the interaction for the combined forces must be checked in accordance with AISC *Specification* (AISC, 2017) Section H1. Bending along the *X*-axis are the values associated with Vierendeel bending and there is no bending stress along the *Y*-axis. Because the axial stress to axial capacity is greater than 0.2, Eqn H1-1a is used. Table 4-6 below is used to organize each element.

$$\frac{P_r}{P_c} + \frac{8}{9}\left(\frac{M_{rx}}{M_{cx}} + \frac{M_{ry}}{M_{cy}}\right) \leq 1.0 \qquad \text{(SPEC Eqn H1-1a)}$$

**Table 4-6 – Interaction Check**

| Opening | $x$, ft | $P_r$ | $P_r/\phi_c P_c$ | $M_{vr}$ | $M_{vr}/\phi_b M_n$ | Spec Eqn | Interaction Value |
|---|---|---|---|---|---|---|---|
| Beam CL | 20.0 | 247.8 | 0.759 | 0.0 | 0.0 | H1-1a | 0.759 |
| 6 | 17.3 | 243.4 | 0.746 | 23.3 | 0.112 | H1-1a | 0.846 |
| 5 | 14.7 | 230.2 | 0.705 | 46.6 | 0.225 | H1-1a | 0.905 |

| | | | | | | | |
|---|---|---|---|---|---|---|---|
| 4 | 12.0 | 208.1 | 0.638 | 69.9 | 0.337 | H1-1a | 0.938 |
| 3 | 9.33 | 177.3 | 0.543 | 93.2 | 0.449 | H1-1a | 0.942 |
| 2 | 6.67 | 137.7 | 0.422 | 116.5 | 0.561 | H1-1a | 0.921 |
| 1 | 4.0 | 89.2 | 0.273 | 139.8 | 0.674 | H1-1a | 0.872 |

Looking at each interaction value, there are no values that exceed 1.0; therefore the tee section meets the strength interaction requirements.

## Web Post Flexural Strength

Shear forces through the web sections creates a moment on the top and bottom section of the web. The magnitude of the horizontal shear is found using DG 31 Eqn 3-19.

$$V_{rh} = \left|\frac{M_{r(i+1)} - M_{r(i)}}{d_{effec}}\right| = \left|T_{r(i)} - T_{r(i+1)}\right| \qquad \text{(DG 31 Eqn 3-19)}$$

Table 4-7 lists each global moment at each opening. Each web uses the difference of moment from adjacent openings. Each shear force is then converted to the web post moment by a moment arm of 12.1 in., which is half the opening height, $h_o$, of 24.2 in.

**Table 4-7 – Horizontal Shear Forces**

| Opening | $x$, ft | $V_r$, k | $M_r$, k-ft | $\Delta M_r$, k-ft | $V_{rh}$, k | $M_u$, k-in |
|---|---|---|---|---|---|---|
| Beam CL | 20.0 | 0.0 | 699.2 | | | |
| 6 | 17.3 | 9.3 | 686.8 | 12.4 | 4.41 | 53.4 |
| 5 | 14.7 | 18.6 | 649.5 | 37.3 | 13.22 | 160.0 |
| 4 | 12.0 | 28 | 587.3 | 62.2 | 22.03 | 266.6 |
| 3 | 9.33 | 37.3 | 500.3 | 87 | 30.84 | 373.2 |
| 2 | 6.67 | 46.6 | 388.4 | 111.9 | 39.65 | 479.8 |

| | | | | | | |
|---|---|---|---|---|---|---|
| 1 | 4.0 | 55.9 | 251.7 | 136.7 | 48.46 | 586.4 |

The design moment strength of the web post varies primarily on the length to thickness ratio and the angle of the hexagonal cut. First the plastic bending moment, *Mp*, of the web posts can be found by using DG 31 Eqn 3-22.

$$M_p = 0.25t_w(e + 2b)^2F_y \qquad \text{(DG 31 Eqn 3-22)}$$

$$M_p = 0.25(0.47\text{ in})\big(10.0\text{ in} + 2(6.0\text{ in})\big)^2 50\text{ ksi} = 2843.5\text{ k} - \text{in}$$

With the angle being 63.6°, the 60° set of equations will be used.

$$\frac{e}{t_w} = \frac{10\text{ in}}{0.47\text{ in}} = 21.3$$

$$\frac{2h}{e} = \frac{2(12.1\text{ in})}{10\text{ in}} = 2.42$$

$$\frac{M_{ocr}}{M_p} = 1.96(0.699)^{2h/e} \qquad \text{(DG 31 Eqn 3-27)}$$

$$\frac{M_{ocr}}{M_p} = 1.96(0.699)^{2.42} = 0.82$$

$$\frac{M_{ocr}}{M_p} = 2.55(0.574)^{2h/e} \qquad \text{(DG 31 Eqn 3-28)}$$

$$\frac{M_{ocr}}{M_p} = 2.55(0.574)^{2.42} = 0.67$$

Interpolation between $e/t_w$ of 20 and 30 is required to find $M_{ocr}/M_p$; however, each value is above the maximum limit of 0.493. The design moment can now be found using DG 31 Eqn 3-29a. The resistance factor, $\phi_b$, is 0.9 since the angle theta is larger than 58°.

$$\phi_b M_n = \phi_b\left(\frac{M_{ocr}}{M_p}\right)M_p \qquad \text{(DG 31 Eqn 3-29a)}$$

$$\phi_b M_n = 0.9(0.493)(2843.5\text{ k} - \text{in}) = 1261.7\text{ k} - \text{in}$$

Comparing to the largest required moment from Table 4-7 of 586 k-in, the web posts local buckling flexural strength is adequate.

## Horizontal Shear Strength

The horizontal shear derived above will be resisted by the weld joining the top and bottom web post sections. The weld strength is assumed to at least match the steel strength. AISC *Specification* (AISC, 2017) Section J4.2 outlines the design strength for elements in shear.

For shear yielding

$$R_n = 0.60F_yA_{gv} \qquad \text{(SPEC Eqn J4-3)}$$

$$\phi = 1.0$$

For shear rupture

$$R_n = 0.60F_uA_{nv} \qquad \text{(SPEC Eqn J4-4)}$$

$$\phi = 0.75$$

Where

$$A_{gv} = A_{nv} = et_w$$

$$et_w = (10\text{ in})(0.47\text{ in}) = 4.7\text{ in}^2$$

For shear yielding

$$\phi R_n = (1.0)0.6(50\text{ ksi})(4.7\text{ in}^2) = 141\text{ k}$$

For shear rupture

$$\phi R_n = (0.75)0.6(65\text{ ksi})(4.7\text{ in}^2) = 137.5\text{ k}$$

Of these two, shear rupture will govern the maximum shear through the web. Looking at horizontal shear from Table 4-7, the maximum shear of 48 k occurs in the web post between the first and second openings. As it is less than the design strength, there is sufficient shear capacity.

## Vertical Shear Strength

The first vertical shear location to be investigated is at the first opening on either end, where the vertical shear is greater than those at other openings. Shear forces are resisted by the top and bottom tee sections. AISC *Specification* (AISC, 2017) Section G3 provides the shear strength for single tee sections, so the total shear strength of the net section will be the sum of top and bottom tees.

$$V_n = 0.6F_y btC_{v2} \qquad \text{(SPEC Eqn G3-1)}$$

Where $C_{v2}$ is defined in Section G2.2

$$\frac{h}{t_w} = \frac{d_t}{t_w}$$

$$K_v = 1.2$$

Finding $C_{v2}$ per Section G2.2

$$\frac{h}{t_w} = \frac{d_t}{t_w} = \frac{6.0 \text{ in}}{0.47 \text{ in}} = 12.77$$

$$1.10\sqrt{\frac{k_v E}{F_y}} = 1.10\sqrt{\frac{1.2(29{,}000 \text{ ksi})}{50 \text{ ksi}}} = 29.02$$

With the height to thickness ratio less than the threshold, $C_{v2}$ shall be determined by Eqn G2-9.

$$C_{v2} = 1.0 \qquad \text{(SPEC Eqn G2-9)}$$

$$V_{n,tee} = 0.6F_y d_t t_w C_{v2}$$

$$V_{n,tee} = 0.6(50 \text{ ksi})(6 \text{ in})(0.47\text{in})(1.0) = 84.6 \text{ k}$$

$$V_n = 2V_{n,tee} = 169.2 \text{ k}$$

Applying the strength reduction factor, $\phi_v$, of 0.9 from Section G1gives

$$\phi_v V_n = 0.9(169.2 \text{ k}) = 152.3 \text{ k}$$

Comparing the design strength to the maximum shear at an opening from Table 4-5 of 56 k, there is ample shear capacity at the net section.

The second vertical shear location is the end reaction through the gross section. AISC *Specification* (AISC, 2017) Section G2.1 outlines the shear strength capacity for I shaped members.

$$V_n = 0.6F_y A_w C_{v1} \qquad \text{(SPEC Eqn G2-1)}$$

To determine $C_{v1}$, the height to depth ratio is examined

$$\frac{h}{t_w} = \frac{d_g - 2k_{des}}{t_w} = \frac{36.2\text{ in} - 2(1.27\text{ in})}{0.47\text{ in}} = 71.62$$

$$1.10\sqrt{\frac{k_v E}{F_y}} = 1.10\sqrt{\frac{5.34(29{,}000\text{ ksi})}{50\text{ ksi}}} = 61.22$$

As the height to depth ratio exceeds the threshold, Eqn G2-4 is used to determine $C_{v1}$.

$$C_{v1} = \frac{1.10\sqrt{k_v E/F_y}}{h/t_w} = \frac{61.22}{71.62} = 0.85 \qquad \text{(SPEC Eqn G2-4)}$$

$$V_n = 0.6(50\text{ ksi})(36.2\text{ in})(0.47\text{ in})(0.85) = 433.9\text{ k}$$

Applying the strength reduction factor, $\phi_v$, of 0.9 from Section G1gives

$$\phi_v V_n = 0.9(433.9\text{ k}) = 390.5\text{ k}$$

Comparing the design strength to the maximum shear from Table 4-5 of 70 k, there is sufficient shear capacity at the gross section.

## Deflection

The last check is for serviceability. For design, live load has an allowable deflection limit of $L/360$ and a total deflection limit of $L/240$. In accordance with DG 31 Section 3.7, the moment of inertia used for deflection calculations will be 90% of the net moment of inertia.

$$0.9I_{x,net} = 0.9(5446\text{ in}^2) = 4901\text{ in}^4$$

The deflection for a simply supported beam is

$$\Delta = \frac{5wL^4}{384\mathrm{EI}}$$

$$\Delta_{LL} = \frac{5(50\text{ psf})(20\text{ ft})(40\text{ ft})^4}{384(29{,}000\text{ ksi})(4901\text{ in}^4)} = 0.034\text{ ft} = 0.41\text{ in}$$

$$\frac{L}{360} = \frac{40\text{ ft}}{360} = 0.11\text{ ft} = 1.33\text{ in}$$

Live load deflection is within the allowable deflection.

$$\Delta_{DL} = \frac{5(79\text{ psf})(20\text{ ft})(40\text{ ft})^4}{384(29{,}000\text{ ksi})(4901\text{ in}^4)} = 0.053\text{ ft} = 0.64\text{ in}$$

$$\Delta_{TL} = \Delta_{LL} + \Delta_{LL}$$

$$\Delta_{TL} = 0.41\text{ in} + 0.64\text{ in} = 1.05\text{ in}$$

$$\frac{L}{240} = \frac{40\text{ ft}}{240} = 0.17\text{ ft} = 2\text{ in}$$

The total deflection is within the allowable deflection, so all serviceability requirements are met.

# Composite Design Example

## Base Section Properties

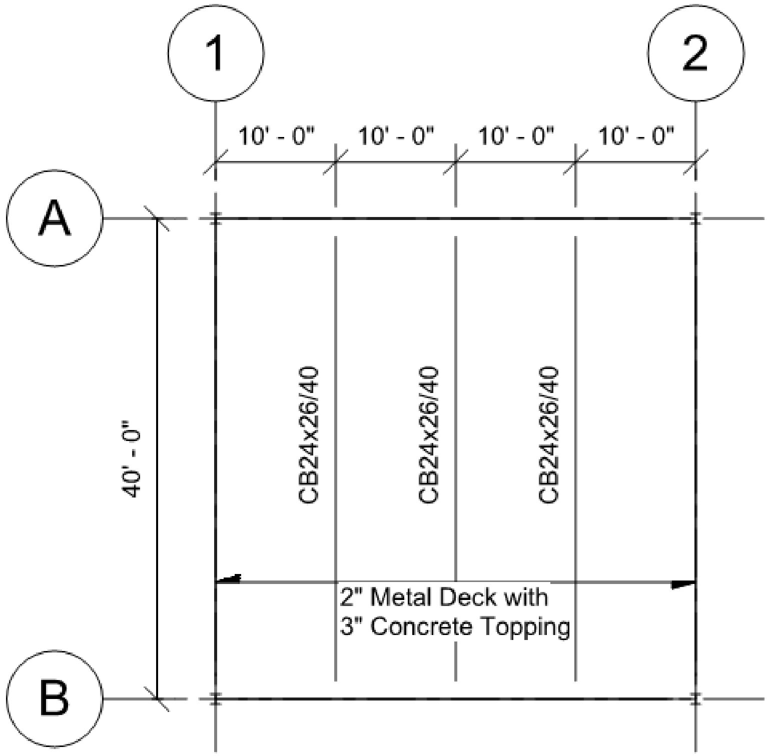


**Figure 4-7 – Composite Bay Floor Plan**

The composite design will use 2VLI19 corrugated floor deck with three-inch thick normal weight concrete topping and four-inch long by ¾" diameter headed studs. The deck system weighs 51 psf and spans 10 feet unshored (Vulcraft, 2008). Assuming the composite beam self-weight to be at most 50 plf, the design dead load over the 10 foot spacing is also five psf. Both beams are idealized to be simply supported. No additional structural loads were considered for the design example.

The first step in the design process is to determine the distributed load on the beam.

$$W_u = 1.2D + 1.6L \qquad \text{(ASCE 7-16 2.3.1.2)}$$

$$W_u = (1.2(51\text{ psf} + 5\text{ psf}) + 1.6(50\text{ psf}))(10\text{ ft spacing}) = 1.47\text{ klf}$$

Next, the base beams can be selected. Initial design looked at a W16x26 and W16x40.

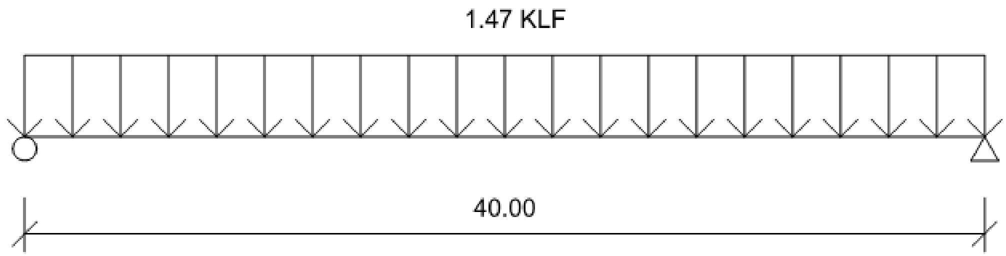


**Figure 4-8 – Beam Loading**

**Table 4-8 – Beam Properties**

| Beam | $A$ | $d$ | $t_w$ | $b_f$ | $t_f$ | $k_{des}$ | $I_x$ | $S_x$ | $Z_x$ |
|---|---|---|---|---|---|---|---|---|---|
| W16x26 | 7.68 | 15.7 | 0.250 | 5.50 | 0.345 | 0.747 | 301 | 38.4 | 44.2 |
| W16x40 | 11.8 | 16.0 | 0.305 | 7.00 | 0.505 | 0.907 | 518 | 64.7 | 73.0 |

With the base beam dimensions known the castellated beam dimensions can be determined. The design used the Peiner-Schnittührung pattern (Grünbauer) as a base, as shown in Figure 4-10. The properties for the CB16x26/40 are listed in Table 4-9. Due to the cutting pattern, the end of the beam has a partial opening. This opening will be filled with a plate.

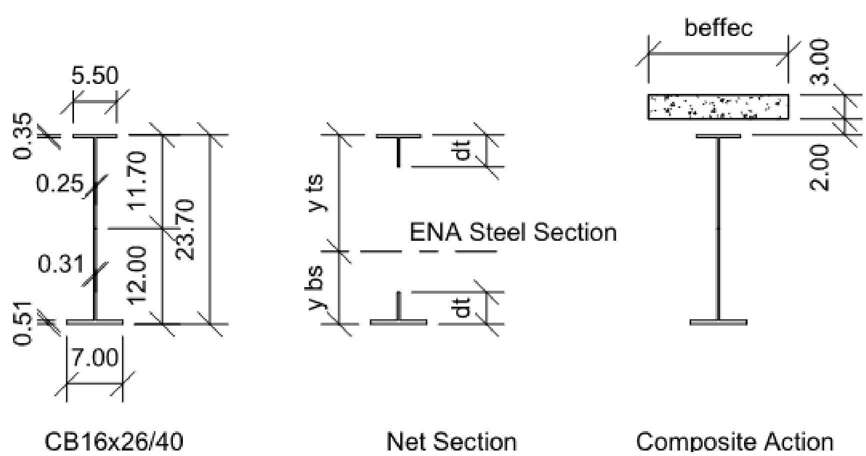


**Figure 4-9 – Composite Castellated Beam Section Dimensions**

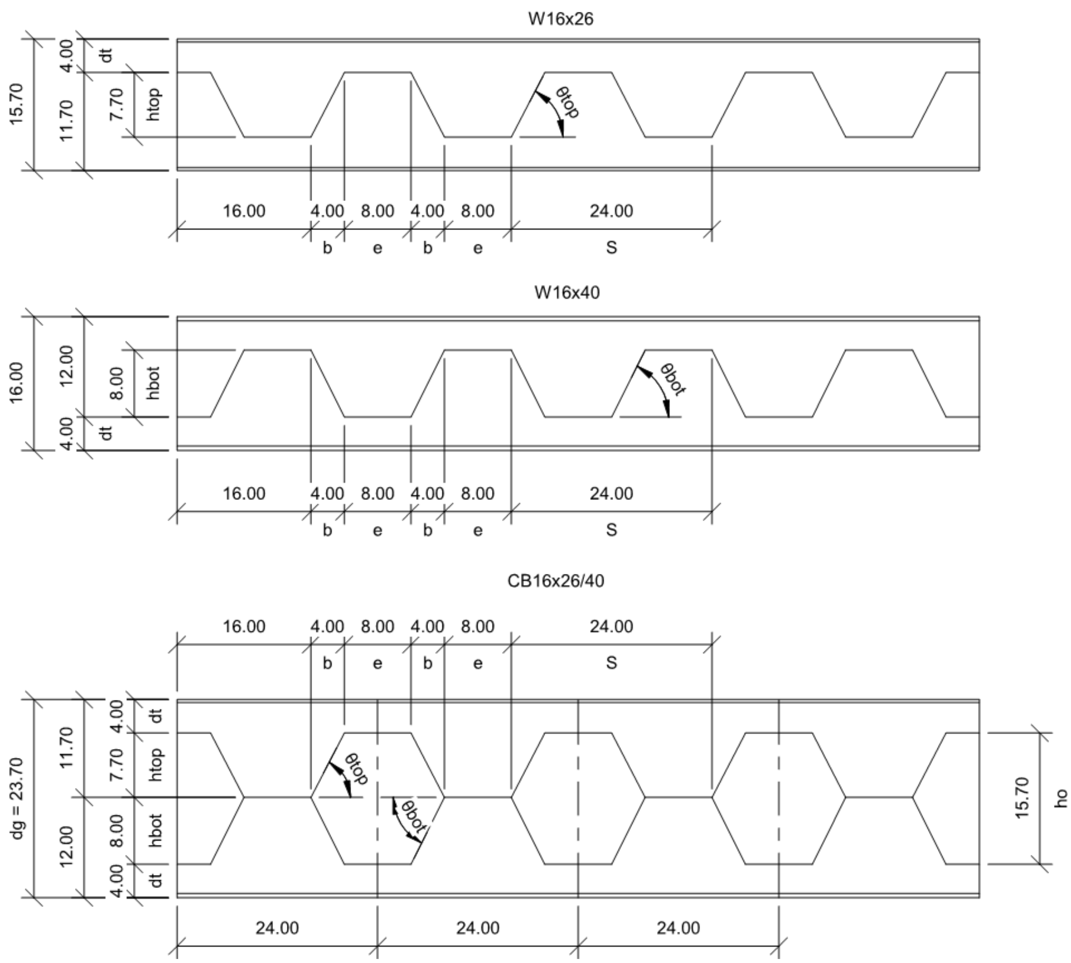


**Figure 4-10 – Castellated Beam Dimensions**

**Table 4-9 – CB16x26/40 Dimensions**

| | | | |
|---|---|---|---|
| $d_g = h_o + 2d_t =$ | 23.7 in | $e =$ | 8 in |
| $b = d/4 =$ | 4.0 in | $d_t = d/4 =$ | 4.0 in |
| $h_{top} = d_{top} - 2d_t =$ | 7.7 in | $h_{bot} = d_{bot} - 2d_t =$ | 8 in |
| $h_o = h_{top} + h_{bot} =$ | 15.7 in | $S = 2(e+b) =$ | 24 in |
| $\theta_{\text{top}} = \tan^{-1}(h_{top}/b) =$ | 62.6° | $\theta_{bot} = \tan^{-1}(h_{bot}/b) =$ | 63.4° |

With the castellated beam openings known, the moment and shear force at each opening can be calculated. The values are listed in Table 4-10. The castellated beam dimensions are also used for the tee sections, whose dimensions are listed in Table 4-11 and shown in Figure 4-11.

**Table 4-10 – Composite Beam Forces**

| Opening | $x$, ft | $V_r$, k | $M_r$, k-ft |
|---|---|---|---|
| Beam CL | 20 | 0.0 | 294.4 |
| 9 | 18 | 2.9 | 291.5 |
| 8 | 16 | 5.9 | 282.6 |
| 7 | 14 | 8.8 | 267.9 |
| 6 | 12 | 11.8 | 247.3 |
| 5 | 10 | 14.7 | 220.8 |
| 4 | 8 | 17.7 | 188.4 |
| 3 | 6 | 20.6 | 150.1 |
| 2 | 4 | 23.6 | 106.0 |
| 1 | 2 | 26.5 | 55.9 |
| Beam End | 0 | 29.4 | 0.0 |

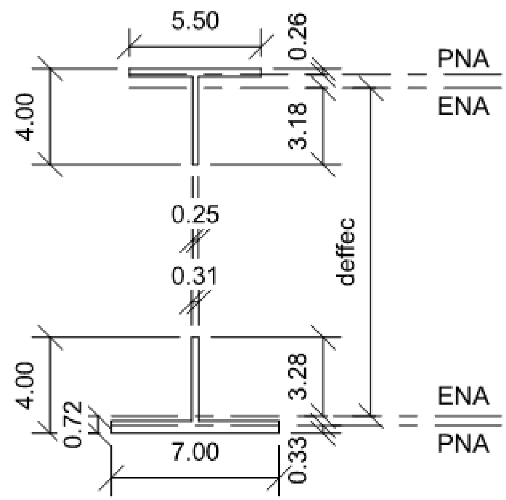


**Figure 4-11 – Tee Section Dimensions**

**Table 4-11 – Tee Section Properties**

| Tee | $A$ | $\bar{y}_{TEE}$ | $I_x$ | $I_y$ | $S_x$ | $S_y$ | $Z_x$ | $Z_y$ | $R_x$ | $R_y$ | $Y_{PNA}$ | $J$ |
|---|---|---|---|---|---|---|---|---|---|---|---|---|
| Top | 2.81 | 3.18 | 3.50 | 4.79 | 1.10 | 1.74 | 1.95 | 2.67 | 1.12 | 1.31 | 0.26 | 0.09 |
| Bot | 4.60 | 0.72 | 4.44 | 14.4 | 1.35 | 4.13 | 0.45 | 6.27 | 0.98 | 1.77 | 0.33 | 0.33 |

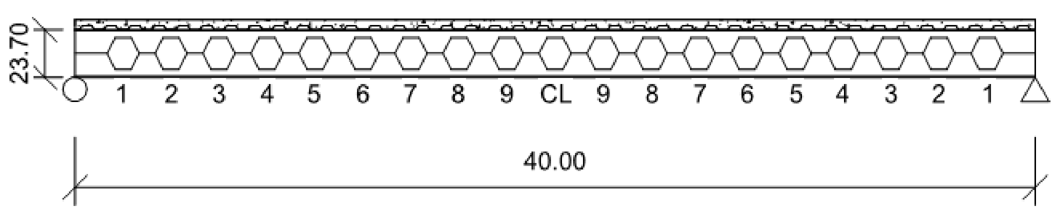


**Figure 4-12 – Castellated Beam Openings**

**Table 4-12 – Web Opening Locations**

| Opening | 1 | 2 | 3 | 4 | 5 | 6 | 7 | 8 | 9 | CL |
|---|---|---|---|---|---|---|---|---|---|---|
| $x$, ft | 2.0 | 4.0 | 6.0 | 8.0 | 10.0 | 12.0 | 14.0 | 16.0 | 18.0 | 20.0 |

Using the tee dimensions and castellated beam opening dimensions, the net section properties can be calculated.

Net section properties

$$A_{net} = A_{Tee,top} + A_{Tee,bot}$$

$$A_{net} = 2.81 \text{ in}^2 + 4.6 \text{ in}^2 = 7.41 \text{ in}^2$$

$$\bar{y}_{bs} = \frac{A_{tee,top}\left(d_t + h_o + \bar{y}_{tee,top}\right) + A_{tee,bot}\bar{y}_{tee,bot}}{A_{net}}$$

$$\bar{y}_{bs} = \frac{(2.81 \text{ in}^2)(4 + 15.7 + 3.18 \text{ in}) + (4.6 \text{ in}^2)(0.72 \text{ in})}{7.41 \text{ in}^2} = 9.12 \text{ in}$$

$$\bar{y}_{ts} = d_g - \bar{y}_{bs}$$

$$\bar{y}_{ts} = 23.7 \text{ in} - 9.12 \text{ in} = 14.58 \text{ in}$$

$$I_{x,net} = I_{x,tee,top} + A_{tee,top}\left[\bar{y}_{ts} - \left(d_t - \bar{y}_{tee,top}\right)\right]^2 + I_{x,tee,bot} + A_{tee,bot}\left(\bar{y}_{bs} - \bar{y}_{tee,bot}\right)^2$$

$$I_{x,net} = 3.5 \text{ in}^4 + 2.81 \text{ in}^2[14.58 \text{ in} - (4 \text{ in} - 3.18 \text{ in})]^2 + 4.44 \text{ in}^4 + 4.6 \text{ in}^2(9.12 \text{ in} - 0.72 \text{ in})^2$$

$$I_{x,net} = 864.6 \text{ in}^4$$

Composite Section Properties

$$n = \frac{E_s}{E_c} = \frac{29{,}000{,}000 \text{ psi}}{33(145 \text{ pcf})^{1.5}\sqrt{3000}} = 9.2$$

$$b_{effec} = min\left(\frac{Span}{4}, Spacing\right)$$

$$b_{effec} = \min\left(\frac{40 \text{ ft}}{4}, 10 \text{ ft}\right)$$

$$b_{effec} = 120 \text{ in}$$

$$A_c = b_{effec}t_c = (120 \text{ in})(3 \text{ in}) = 360 \text{ in}^2$$

$$A_{ctr} = \frac{A_c}{n} = \frac{360 \text{ in}^2}{9.2} = 39.13 \text{ in}^2$$

$$K_c = \frac{A_{ctr}}{A_{ctr} + A_{net}} = \frac{39.13 \text{ in}^2}{39.13 \text{ in}^2 + 7.41 \text{ in}^2} = 0.84$$

$$e_c = h_r + \frac{t_c}{2} = 2 \text{ in} + \frac{3 \text{ in}}{2} = 3.5 \text{ in}$$

Assuming the neutral axis is in the concrete slab

$$y_{cc} = \left(\frac{A_{net}t_c}{A_{ctr}}\right)\left[\sqrt{1 + \frac{2A_{ctr}}{A_{net}t_c}\left(\overline{y}_{ts} + e_c + \frac{t_c}{2}\right)} - 1\right]$$

$$y_{cc} = \left[\frac{(7.41\ \text{in}^2)(3\ \text{in})}{39.13\ \text{in}^2}\right]\left[\sqrt{1 + \frac{2(39.13\ \text{in}^2)}{(7.41\ \text{in}^2)(3\ \text{in})}\left(14.58\ \text{in} + 3.5\ \text{in} + \frac{3\ \text{in}}{2}\right)} - 1\right] = 4.18\ \text{in}$$

$$t_c + h_r = 3\ \text{in} + 2\ \text{in} = 5\ \text{in}$$

Since $y_{cc} < t_c + h_r$, the neutral axis is in the concrete, so the assumption is correct.

$$\overline{y}_c = \left(\overline{y}_{ts} + e_c\right)K_c$$

$$\overline{y}_c = (14.58\ \text{in} + 3.5\ \text{in})0.84 = 15.19\ \text{in}$$

$$I_{x,comp} = \left(\overline{y}_{ts} + e_c\right)\overline{y}_c A_{net} + I_{x,net} + \frac{A_{ctr}{t_c}^2}{12}$$

$$I_{x,comp} = (14.58\ \text{in} + 3.5\ \text{in})(15.19\ \text{in})(7.4\ \text{in}^2) + 864.6\ \text{in}^4 + \frac{(39.13\ \text{in}^2)(3\ \text{in})^2}{12}$$

$$I_{x,comp} = 2926\ \text{in}^4$$

For the first iteration of effective composite depth

$$d_{effec,comp} = d_g - \overline{y}_{tee,bot} + h_r + 0.5t_c$$

$$d_{effec,comp} = 23.7\ \text{in} - 0.72\ \text{in} + 2\ \text{in} + 0.5(3\ \text{in}) = 26.5\ \text{in}$$

## Composite Action

Calculate the shear strength of the concrete slab.

$$V_c = \Phi_{cv}V_{nc}$$

$$V_c = \Phi_{cv}4\sqrt{f_c{}'}(3)(h_r + t_c)t_c$$

$$V_c = 0.75(4)\sqrt{3000\ \text{psi}}(3)(2\ \text{in} + 3\ \text{in})(3\ \text{in}) = 7.39\ \text{k}$$

To find the axial forces on the tees, the effective composite depth is rechecked until the change is minimal.

$$T_{1(i)} = C_{1(i)} = \frac{M_{r(i)}}{d_{effec,comp}}$$

$$X_c = \frac{C_{1(i)}}{0.85 f_c' b_{effec}}$$

$$d_{effec,comp} = d_g - \overline{y}_{tee,bot} + h_r - \frac{X_c}{2}$$

**Table 4-13 – Axial Forces Iteration**

| Opening Number | $x$,ft | $M_r$, k-ft | $C_{1(i)}$ | $X_{c(i)}$ | $d_{effec}$ | $C_{1(i+1)}$ | $X_{c(i+1)}$ | $d_{effec}$ | $C_{1(i+2)}$ | $C_{(i+1)}/C_{(i+2)}$ |
|---|---|---|---|---|---|---|---|---|---|---|
| Beam CL | 20 | 294.4 | 133.4 | 0.436 | 27.77 | 127.2 | 0.416 | 27.78 | 127.2 | 1.00 |
| 9 | 18 | 291.5 | 132.1 | 0.432 | 27.77 | 126.0 | 0.412 | 27.78 | 125.9 | 1.00 |
| 8 | 16 | 282.6 | 128.1 | 0.418 | 27.77 | 122.1 | 0.399 | 27.78 | 122.1 | 1.00 |
| 7 | 14 | 267.9 | 121.4 | 0.397 | 27.79 | 115.7 | 0.378 | 27.80 | 115.7 | 1.00 |
| 6 | 12 | 247.3 | 112.1 | 0.366 | 27.80 | 106.7 | 0.349 | 27.81 | 106.7 | 1.00 |
| 5 | 10 | 220.8 | 100.0 | 0.327 | 27.82 | 95.2 | 0.311 | 27.83 | 95.2 | 1.00 |
| 4 | 8 | 188.4 | 85.4 | 0.279 | 27.84 | 81.2 | 0.265 | 27.85 | 81.2 | 1.00 |
| 3 | 6 | 150.1 | 68.0 | 0.222 | 27.87 | 64.6 | 0.211 | 27.88 | 64.6 | 1.00 |
| 2 | 4 | 106.0 | 48.0 | 0.157 | 27.91 | 45.6 | 0.149 | 27.91 | 45.6 | 1.00 |
| 1 | 2 | 55.9 | 25.3 | 0.083 | 27.94 | 24.0 | 0.079 | 27.94 | 24.0 | 1.00 |
| Beam End | 0 | 0.0 | 0.0 | 0.0 | 27.984 | 0.0 | 0.0 | 27.984 | 0.0 | 1.00 |

With the new axial forces, the number of studs for full composite action can be found. If fewer studs are used, sections of the beam will be partially composite and the top tee section will have an axial force, $T_o$. From AISC *Specification* (AISC, 2017) Section I3.2d.1 the shear transfer is limited by concrete crushing and tensile yielding of the steel net section.

Concrete crushing

$$V' = 0.85 f_c' A_c \qquad \text{(SPEC Eqn I3-1a)}$$

$$V' = 0.85(3000\text{ psi})(360\text{ in}^2) = 918\text{ k}$$

Tensile Yielding

$$V' = F_y A_s \qquad \text{(SPEC Eqn I3-1b)}$$

$$V' = (50\text{ ksi})(7.41\text{ in}^2) = 370.5\text{ k}$$

Tensile yielding governs the shear capacity. The shear capacity for a single stud is found in AISC *Steel Construction Manual* (AISC, 2017) Table 3-21. Design capacity studs are perpendicular to the deck and are considered strong.

$$Q_n = 21\text{ kips/stud}$$

$$N = \frac{V'}{Q_n} = \frac{370.5\text{ k}}{21\text{ k/stud}} = 18\text{ studs}$$

Between the maximum moment at midspan and the end of the beam, 18 studs need to be provided. As the beam length is 40 feet, each stud can be in its own flute at one foot spacing. The average stud shear density is then

$$q = \frac{2(V\ provided)}{Beam\ Span} = \frac{2(18\text{ studs})(21\text{ k/stud})}{40\text{ ft}} = 18.9\text{ k/ft}$$

Next the axial forces are compared to the concrete capacity developed by the anchor studs. If the axial force is greater than the stud force, the opening is only partially composite and the top tee withstands leftover compression forces.

For partial composite, the axial forces are given by DG 31 Eqn 3-12 and Eqn 3-13. The top tee will experience a compressive force, $T_o$.

$$T_o = M_r\left[\frac{1-\frac{q(X_i)}{T_{1(i+2)}}}{d_{effec}}\right] \quad \text{(DG 31 Eqn 3-12)}$$

$$d_{effec} = d_g - \left[\left(d_t - \overline{y}_{tee,top}\right) + \overline{y}_{tee,bot}\right]$$

The bottom tee will experience a new tensile force, $T_{1,new}$.

$$T_{1,new} = qX_i + T_o \quad \text{(DG 31 Eqn 3-13)}$$

**Table 4-14 – Revised Local Axial Forces**

| Opening Number | $x$, ft | $T_{1(i+2)}$, k | $qXi$, k | Composite Status | $T_o$, k | $T_{1,new}$, k |
|---|---|---|---|---|---|---|
| Beam CL | 20 | 127.2 | 378 | Full | 0 | 127.2 |
| 9 | 18 | 125.9 | 340.2 | Full | 0 | 125.9 |
| 8 | 16 | 122.1 | 302.4 | Full | 0 | 122.1 |
| 7 | 14 | 115.7 | 264.6 | Full | 0 | 115.7 |
| 6 | 12 | 106.7 | 226.8 | Full | 0 | 106.7 |
| 5 | 10 | 95.2 | 189 | Full | 0 | 95.2 |
| 4 | 8 | 81.2 | 151.2 | Full | 0 | 81.2 |
| 3 | 6 | 64.6 | 113.4 | Full | 0 | 64.6 |
| 2 | 4 | 45.6 | 75.6 | Full | 0 | 45.6 |
| 1 | 2 | 24.0 | 37.8 | Full | 0 | 24.0 |
| Beam End | 0 | 0 | 0 | Full | 0 | 0 |

## Tee Axial Strength

Since the composite beam has full composite action, no tee section experiences compression. The only axial force acting on a tee section is the $T_{1,new}$ force on the bottom tee. Since the tee area is the same for both rupture and yielding, tensile yielding will always govern. AISC *Specification* (AISC, 2017) Eqn D2-1 is used.

$$\Phi_t P_n = \Phi_t F_y A_g \qquad \text{(SPEC Eqn D2-1)}$$

$$\Phi_t P_n = (0.9)(50 \text{ ksi})(4.6 \text{ in}^2) = 207 \text{ k}$$

Comparing the 207 k tensile capacity to the new axial force of 127 k at midspan from Table 4-14, there is sufficient capacity at each section.

## Tee Flexural Strength

The Vierendeel moment experienced by the tees is caused by the net shear force, which is found by reducing the global shear by the shear capacity of the concrete slab. The shear forces are then distributed to either tee section proportioned by area.

$$M_{vr,top} = V_{net} \frac{A_{tee,top}}{A_{net}} \left(\frac{e}{2}\right) \qquad \text{(SPEC Eqn 3-2)}$$

$$M_{vr,bot} = V_{net} \frac{A_{tee,bot}}{A_{net}} \left(\frac{e}{2}\right) \qquad \text{(SPEC Eqn 3-2)}$$

**Table 4-15 – Vierendeel Moment**

| Opening Number | $x$, ft | $V_{net}$, k | $M_{vr,top}$, k-in | $M_{vr,bot}$, k-in |
|---|---|---|---|---|
| Beam CL | 20 | 0.0 | 0.0 | 0.0 |
| 9 | 18 | 0.0 | 0.0 | 0.0 |
| 8 | 16 | 0.0 | 0.0 | 0.0 |
| 7 | 14 | 1.44 | 2.18 | 3.57 |
| 6 | 12 | 4.38 | 6.65 | 10.88 |
| 5 | 10 | 7.33 | 11.11 | 18.19 |
| 4 | 8 | 10.27 | 15.58 | 25.50 |
| 3 | 6 | 13.21 | 20.05 | 32.81 |
| 2 | 4 | 16.16 | 24.51 | 40.12 |
| 1 | 2 | 19.10 | 28.98 | 47.43 |

AISC *Specification* (AISC, 2017) Section F9 outlines the moment capacity of tee sections. The first limit case is yielding.

Tee Flexural Yielding

$$M_n = M_p \qquad \text{(SPEC Eqn F9-1)}$$

For both tee sections, the tee stems are conservatively assumed to be under compression forces. Eqn F9-4 is used.

$$M_p = M_y \qquad \text{(SPEC Eqn F9-4)}$$

$$M_y = F_y S_x \qquad \text{(SPEC Eqn F9-3)}$$

$$M_{y,top} = (50\text{ ksi})(1.1\text{ in}^3) = 55\text{ k} - \text{in}$$

$$M_{y,bot} = (50\text{ ksi})(1.35\text{ in}^3) = 67.5\text{ k} - \text{in}$$

Lateral-Torsional Buckling

Each tee section is unbraced for a distance e. AISC *Specification* (AISC, 2017) F9.2 is used to check for lateral-torsional buckling capacity. The length of the tee section, *e*, is compared to the limiting laterally unbraced length $L_b$.

$$L_b = 1.76 r_y \sqrt{\frac{E}{F_y}} \qquad \text{(SPEC Eqn F9-8)}$$

$$L_{b,top} = 1.76(1.31\text{ in})\sqrt{\frac{29{,}000\text{ ksi}}{50\text{ ksi}}} = 55.5\text{ in}$$

$$L_{b,bot} = 1.76(1.77\text{ in})\sqrt{\frac{29{,}000\text{ ksi}}{50\text{ ksi}}} = 75.0\text{ in}$$

As both limiting laterally unbraced length are greater than the length of the tee section, *e*, lateral-torsional buckling does not apply.

Flange Local Buckling

Check limiting flange width-to-thickness ratio per AISC *Specification* (AISC, 2017) Table B4.1b, Case 10.

$$\lambda_p = 0.38\sqrt{\frac{E}{F_y}} = 0.38\sqrt{\frac{29{,}000{,}000 \text{ psi}}{50{,}000 \text{ psi}}} = 9.15$$

$$\lambda_r = 1.0\sqrt{\frac{E}{F_y}} = 1.0\sqrt{\frac{29{,}000{,}000 \text{ psi}}{50{,}000 \text{ psi}}} = 24.08$$

$$\lambda_{top} = \frac{b}{t} = \frac{b_f}{2t_f} = \frac{5.5 \text{ in}}{2(0.345 \text{ in})} = 7.97$$

$$\lambda_{bot} = \frac{b}{t} = \frac{b_f}{2t_f} = \frac{7 \text{ in}}{2(0.505 \text{ in})} = 6.93$$

Both flanges are compact, so flange local buckling does not govern.

Tee Stem Local Buckling

Eqn F9-16 limits the strength due to tee stem local buckling.

$$M_n = F_{cr}S_x$$

The critical force depends on the length to thickness ratio.

$$\frac{d}{t_w} = \frac{d_t}{t_w} = \frac{4 \text{ in}}{0.25 \text{ in}} = 16$$

$$0.84\sqrt{\frac{E}{F_y}} = 0.84\sqrt{\frac{29{,}000 \text{ kis}}{50 \text{ ksi}}} = 20.23$$

As the length to thickness ratio of the top tee is less than the first threshold, Eqn F9-17 determines the value of the critical stress. The bottom tee will also be governed by Eqn F9-17 as it has a thicker web.

$$F_{cr} = F_y$$

$$F_{cr} = 50 \text{ ksi}$$

$$M_{y,top} = (50\text{ ksi})(1.1\text{ in}^3) = 55\text{ k} - \text{in}$$

$$M_{y,bot} = (50\text{ ksi})(1.35\text{ in}^3) = 67.5\text{ k} - \text{in}$$

The smallest nominal moment will be used from the four limit states. For this example, $M_{n,top}$ is taken as 55 k-in and $M_{n,bot}$ as 67.5 k-in. Substituting into Eqn F9-1 and applying the resistance factor, $\phi_b$, of 0.9 from Section F1 gives the flexural yielding strength.

$$\phi_b M_{n,top} = \phi_b M_{y,top} = 0.9(55\text{ k} - \text{in}) = 49.5\text{ k} - \text{in}$$

$$\phi_b M_{n,bot} = \phi_b M_{y,bot} = 0.9(67.5\text{ k} - \text{in}) = 60.75\text{ k} - \text{in}$$

From Table 4-15, the maximum Vierendeel moment experienced is 29 k-in at the top and 47 k-in at the bottom tee, both of which are under the design capacity. No value is listed at the beam end because there is no tee section from an opening there.

## Combined Forces

With both axial and flexural forces acting on the tee section, the interaction for the combined forces must be checked in accordance with AISC *Specification* (2017) Chapter H1. The axial force ratio determines if Eqn H1-1a or H1-1b is used. As the axial force varies at each location, both equations may be used. Table 4-14 below is used to organize each element to quickly apply either equation. Bending along the *X*-axis are the values associated with Vierendeel bending and there is no bending stress along the *Y*-axis.

$$\frac{P_r}{P_c} + \frac{8}{9}\left(\frac{M_{rx}}{M_{cx}} + \frac{M_{ry}}{M_{cy}}\right) \leq 1.0 \qquad \text{(SPEC Eqn H1-1a)}$$

$$\frac{\mathrm{P_r}}{2\mathrm{P_c}} + \left(\frac{\mathrm{M_{rx}}}{\mathrm{M_{cx}}} + \frac{\mathrm{M_{ry}}}{\mathrm{M_{cy}}}\right) \leq 1.0 \qquad \text{(SPEC Eqn H1-1b)}$$

**Table 4-16 – Bottom Tee Interaction Check**

| Opening | $x$, ft | Bot Tee | | | | Interaction Value |
|---|---|---|---|---|---|---|
| | | $P_r$ | $P_r/\phi_c P_c$ | $M_{vr}$ | $M_{vr}/\phi_b M_n$ | |
| Beam CL | 20 | 127 | 0.61 | 0.0 | 0.0 | 0.61 |
| 9 | 18 | 126 | 0.61 | 0.0 | 0.0 | 0.61 |
| 8 | 16 | 122 | 0.59 | 0.0 | 0.0 | 0.59 |
| 7 | 14 | 116 | 0.56 | 3.57 | 0.06 | 0.61 |
| 6 | 12 | 107 | 0.52 | 10.88 | 0.18 | 0.67 |
| 5 | 10 | 95.2 | 0.46 | 18.19 | 0.30 | 0.73 |
| 4 | 8 | 81.2 | 0.39 | 25.50 | 0.42 | 0.76 |
| 3 | 6 | 64.6 | 0.31 | 32.81 | 0.54 | 0.79 |
| 2 | 4 | 45.6 | 0.22 | 40.12 | 0.66 | 0.81 |
| 1 | 2 | 24.0 | 0.12 | 47.43 | 0.78 | 0.84 |

Looking at each interaction value, there are no values that exceed 1.0; therefore the tee section meets the stress interaction requirements.

## Web Post Flexural Strength

Shear forces through the web sections creates a moment on the top and bottom section of the web. The magnitude of the horizontal shear is found using DG 31 Eqn 3-19.

$$V_{rh} = \left|T_{r(i)} - T_{r(i+1)}\right| \qquad \text{(DG 31 Eqn 3-19)}$$

Table 4-17 lists each axial force. Each web uses the difference of axial forces from adjacent openings.

**Table 4-17 – Horizontal Shear Forces**

| Opening | $x$, ft | $T_{r(i)}$ | $T_{r(i+1)}$ | $V_{rh} = \Delta T_r$ |
|---|---|---|---|---|
| Beam CL | 20 | 127.19 | | |
| 9 | 18 | 125.91 | 127.19 | 1.28 |
| 8 | 16 | 122.06 | 125.91 | 3.84 |
| 7 | 14 | 115.66 | 122.06 | 6.40 |
| 6 | 12 | 106.71 | 115.66 | 8.95 |
| 5 | 10 | 95.21 | 106.71 | 11.50 |
| 4 | 8 | 81.18 | 95.21 | 14.03 |
| 3 | 6 | 64.63 | 81.18 | 16.55 |
| 2 | 4 | 45.57 | 64.63 | 19.06 |
| 1 | 2 | 24.02 | 45.57 | 21.55 |

The horizontal shear acts at a moment arm equal to either web post height to create the web post moments.

$$M_u = hV_{rh}$$

$$M_{u,top} = (7.7 \text{ in})(21.55 \text{ k}) = 165.9 \text{ k} - \text{in}$$

$$M_{u,bot} = (8 \text{ in})(21.55 \text{ k}) = 172.4 \text{ k} - \text{in}$$

The design moment strength of the web post varies primarily on the width to thickness ratio and the angle of the hexagonal cut. First the plastic bending moment, *Mp*, of the web posts is found by using DG 31 Eqn 3-22.

$$M_p = 0.25t_w(e + 2b)^2F_y \qquad \text{(DG 31 Eqn 3-22)}$$

$$M_{p,top} = 0.25(0.25 \text{ in})\big(8 \text{ in} + 2(4 \text{ in})\big)^2 50 \text{ ksi} = 800 \text{ k} - \text{in}$$

$$M_{p,bot} = 0.25(0.305\text{ in})\big(8\text{ in} + 2(4\text{ in})\big)^2 50\text{ ksi} = 976\text{ k} - \text{in}$$

Each theta is over 60°, so the 60° set of equations will be used. First the top web post is examined.

$$\frac{e}{t_w} = \frac{8\text{ in}}{0.25\text{ in}} = 32$$

$$\frac{2h}{e} = \frac{2(7.7\text{ in})}{8\text{ in}} = 1.925$$

$$\frac{M_{ocr}}{M_p} = 2.55(0.574)^{2h/e} \qquad \text{(DG 31 Eqn 3-28)}$$

$$\frac{M_{ocr}}{M_p} = 2.55(0.574)^{1.93} = 0.88 \leq 0.493$$

The design moment can now be found using DG 31 Eqn 3-29a. The resistance factor, $\phi_b$, is 0.9 since the angle theta is larger than 58°.

$$\phi M_n = \phi_b \left(\frac{M_{ocr}}{M_p}\right) M_p \qquad \text{(DG 31 Eqn 3-29a)}$$

$$\phi M_n = 0.9(0.493)(800\text{ k} - \text{in}) = 355.0\text{ k} - \text{in}$$

Comparing the design moment to the top web post moment of 166 k-in, there is sufficient buckling capacity in the top web posts. Now the bottom web post is investigated.

$$\frac{e}{t_w} = \frac{8\text{ in}}{0.305\text{ in}} = 26.2$$

$$\frac{2h}{e} = \frac{2(8\text{ in})}{8\text{ in}} = 2$$

$$\frac{M_{ocr}}{M_p} = 1.96(0.699)^{2h/e} \qquad \text{(DG 31 Eqn 3-27)}$$

$$\frac{M_{ocr}}{M_p} = 1.96(0.699)^2 = 0.96 \leq 0.493$$

$$\frac{M_{ocr}}{M_p} = 2.55(0.574)^{2h/e} \qquad \text{(DG 31 Eqn 3-28)}$$

$$\frac{M_{ocr}}{M_p} = 2.55(0.574)^2 = 0.84 \ \leq 0.493$$

As the thickness to length ratio falls between 20 and 30, interpolation would be required if the reduction was less than the permitted 0.493 limit. The design moment can now be found using DG 31 Eqn 3-29a. The resistance factor, $\phi_b$, is 0.9 since the angle theta is larger than 58°.

$$\phi M_n = 0.9(0.493)(976 \text{ k} - \text{in}) = 433.1 \text{ k} - \text{in}$$

Comparing the design moment to the top web post moment of 172 k-in, there is sufficient buckling capacity in the bottom web posts.

## Horizontal Shear Strength

The horizontal shear derived in the web post buckling section will be resisted by the weld joining the top and bottom web sections. The weld strength is assumed to at least match the steel strength. AISC *Specification* (AISC, 2017) Section J4.2 outlines the design strength for elements in shear. The web thickness of the top tee section is used as it is the smaller thickness.

For shear yielding

$$R_n = 0.60F_yA_{gv} \qquad \text{(SPEC Eqn J4-3)}$$

$$\phi = 1.0$$

For shear rupture

$$R_n = 0.60F_uA_{nv} \qquad \text{(SPEC Eqn J4-4)}$$

$$\phi = 0.75$$

$$A_{gv} = A_{nv} = et_w$$

$$et_w = (8 \text{ in})(0.25 \text{ in}) = 2 \text{ in}^2$$

For shear yielding

$$\phi R_n = (1.0)0.6(50 \text{ ksi})(2 \text{ in}^2) = 60 \text{ k}$$

For shear rupture

$$\phi R_n = (0.75)0.6(65 \text{ ksi})(2 \text{ in}^2) = 58.5 \text{ k}$$

Of these two, shear rupture will govern the shear strength of the web. Looking at horizontal shear from 4-17, the maximum shear of 21.5 k occurs in the web post between the first and second openings. As it is less than the design strength, there is sufficient shear capacity.

## Vertical Shear Strength

The first vertical shear location to be investigated is at the first opening on either end. From Table 4-10, the shear at the first opening is 26.5 k. With the opening, the global shear force is resisted by the top and bottom tee sections. AISC *Specificatio*n (AISC, 2017) Section G3 provides the shear strength for single tee sections. For this asymmetric beam, both sections will need to be calculated. Starting with the top tee section,

$$V_{u,top} = V_u \left( \frac{A_{tee,top}}{A_{net}} \right)$$

$$V_{u,top} = (26.5 \text{ k}) \left( \frac{2.81 \text{ in}^2}{7.41 \text{ in}^2} \right) = 10.1 \text{ k}$$

$$V_n = 0.6 F_y b t C_{v2} \qquad \text{(SPEC Eqn G3-1)}$$

Where $C_{v2}$ is defined in Section G2.2 using

$$\frac{h}{t_w} = \frac{d_t}{t_w}$$

$$K_v = 1.2$$

Finding $C_{v2}$ per Section G2.2

$$\frac{h}{t_w} = \frac{d_t}{t_w} = \frac{4 \text{ in}}{0.25 \text{ in}} = 16$$

$$1.10\sqrt{\frac{k_v E}{F_y}} = 1.10\sqrt{\frac{1.2(29{,}000\text{ ksi})}{50\text{ ksi}}} = 29.02$$

With the height to thickness ratio less than the threshold, $C_{v2}$ shall be determined by Eqn G2-9.

$$C_{v2} = 1.0 \qquad \text{(SPEC Eqn G2-9)}$$

$$V_{n,tee,top} = 0.6F_y d_t t_w C_{v2}$$

$$V_{n,tee} = 0.6(50\text{ ksi})(4\text{ in})(0.25\text{ in})(1.0) = 30\text{ k}$$

Applying the strength reduction factor, $\phi_v$, of 0.9 from Section G1gives

$$\phi_v V_n = 0.9(30\text{ k}) = 27\text{ k}$$

The design strength is larger than the 10.1 k experienced by the top tee. Next, the bottom tee section is checked.

$$V_{u,bot} = V_u\left(\frac{A_{tee,bot}}{A_{net}}\right)$$

$$V_{u,bot} = (26.5\text{ k})\left(\frac{4.6\text{ in}^2}{7.41\text{ in}^2}\right) = 16.5\text{ k}$$

$$V_n = 0.6F_y b t C_{v2} \qquad \text{(SPEC Eqn G3-1)}$$

Where $C_{v2}$ is defined in Section G2.2

$$\frac{h}{t_w} = \frac{d_t}{t_w}$$

$$K_v = 1.2$$

Finding $C_{v2}$ per Section G2.2

$$\frac{h}{t_w} = \frac{d_t}{t_w} = \frac{4\text{ in}}{0.305\text{ in}} = 13.11$$

$$1.10\sqrt{\frac{k_v E}{F_y}} = 1.10\sqrt{\frac{1.2(29{,}000\text{ ksi})}{50\text{ ksi}}} = 29.02$$

With the height to thickness ratio less than the threshold, $C_{v2}$ shall be determined by Eqn G2-9.

$$C_{v2} = 1.0 \qquad \text{(SPEC Eqn G2-9)}$$

$$V_{n,tee} = 0.6F_y d_t t_w C_{v2}$$

$$V_{n,tee} = 0.6(50\text{ ksi})(4\text{ in})(0.305\text{ in})(1.0) = 36.6\text{ k}$$

Applying the strength reduction factor, $\phi_v$, of 0.9 from Section G1gives

$$\phi_v V_n = 0.9(36.6\text{ k}) = 32.9\text{ k}$$

The design capacity for shear is larger than the 16.5 k experienced by the bottom tee. Both tee sections have sufficient shear capacity at the net section.

The second vertical shear location is the end reaction through the gross section. The smaller of the two web thicknesses will be used. AISC *Specification* (AISC, 2017) Section G2.1 outlines the shear strength capacity for I shaped members.

$$V_n = 0.6F_y A_w C_{v1} \qquad \text{(SPEC Eqn G2-1)}$$

To determine $C_{v1}$, the height to depth ratio is examined

$$\frac{h}{t_w} = \frac{d_g - k_{des,top} - k_{des,bot}}{t_w} = \frac{23.7\text{ in} - 0.75\text{ in} - 0.91\text{ in}}{0.25\text{ in}} = 88.16$$

$$1.10\sqrt{\frac{k_v E}{F_y}} = 1.10\sqrt{\frac{5.34(29{,}000\text{ ksi})}{50\text{ ksi}}} = 61.22$$

As the height to depth ratio exceeds the threshold, Eqn G2-4 is used to determine $C_{v1}$.

$$C_{v1} = \frac{1.10\sqrt{k_v E/F_y}}{h/t_w} = \frac{61.22}{88.18} = 0.694 \qquad \text{(SPEC Eqn G2-4)}$$

$$V_n = 0.6(50\text{ ksi})(23.7\text{ in})(0.25\text{ in})(0.694) = 123.4\text{ k}$$

Applying the strength reduction factor, $\phi_v$, of 0.9 from Section G1gives

$$\phi_v V_n = 0.9(123.4\text{ k}) = 111.1\text{ k}$$

Comparing the design strength to the maximum shear from Table 4-9 of 29.4 k, there is sufficient shear capacity at the gross section.

## Deflection

The last check is for serviceability. Before the composite moment of inertia is used, the dead load for pre-composite action is checked. For design, live load has an allowable deflection limit of *L*/360 and a total deflection limit of *L*/240. In accordance with DG 31 Section 3.7, the moment of inertia used for deflection calculations will be 90% of the net moment of inertia.

$$0.9I_{x,net} = 0.9(864.6\ \text{in}^2) = 778.1\ \text{in}^4$$

$$0.9I_{x,comp} = 0.9(2926\ \text{in}^2) = 2633\ \text{in}^4$$

The pre-composite dead load deflection is

$$\Delta = \frac{5wL^4}{384\text{EI}}$$

$$\Delta_{PDL} = \frac{5(56\ \text{psf})(10\ \text{ft})(40\ \text{ft})^4}{384(29{,}000\ \text{ksi})(778.1\ \text{in}^4)} = 0.12\ \text{ft} = 1.43\ \text{in}$$

With a 1.43-inch pre-composite deflection, a 1.25-inch camber can be used.

Live load deflection is

$$\Delta_{LL} = \frac{5(50\ \text{psf})(10\ \text{ft})(40\ \text{ft})^4}{384(29{,}000\ \text{ksi})(2633\ \text{in}^4)} = 0.03\ \text{ft} = 0.38\ \text{in}$$

$$\frac{L}{360} = \frac{40\ \text{ft}}{360} = 0.11\ \text{ft} = 1.33\ \text{in}$$

Live load deflection is within the allowable deflection.

$$\Delta_{TL} = \Delta_{LL} + \Delta_{DL} - camber$$

$$\Delta_{TL} = 0.38\ \text{in} + 1.43\ \text{in} - 1.25\ \text{in} = 0.56\ \text{in}$$

$$\frac{L}{240} = \frac{40\ \text{ft}}{240} = 0.17\ \text{ft} = 2\ \text{in}$$

The total deflection is within the allowable deflection, so all serviceability requirements are met.

# Chapter 5 – Conclusion

Castellated steel beams are an efficient member and can increase strength and stiffness significantly whiling reducing total structural weight. Castellated beams work efficiently for relatively long spans. However, due to the existence of web openings, castellated beams behave differently than solid web W-shape beams, and are more complicated to design. Discontinuity around web openings causes new local load effects, such as Vierendeel bending and web post buckling.

When designing castellated beams, a base beam, or two base beams for asymmetric design, must be selected along with a cutting pattern. Then the properties of the castellated beam are calculated accordingly in order to check various limit states. In addition to global limit states similar to traditional I-beams, there are local limit states that must be investigated. These local limit states arise from transferring the loading forces around the web opening. The magnitude of the forces and design capacity are dependent on the dimensions of the web opening which are determined by the cutting pattern. Major local load effects include the Vierendeel moments developed in the tees above and below the openings, and moments developed in web posts between openings due to the horizontal shear. Most strength calculations follow AISC *Specification for Structural Steel Buildings* (AISC, 2017) while some empirical equations were developed from previous studies for strengths of local effect limit states, such as web post flexural strength due to local buckling. When strengths of some limit states are found to be inadequate, the base beam can be upsized, or the cutting pattern dimensions can be adjusted to obtain adequate strength.

In addition to the new local limit states, the limit states for global forces must also be checked. The global forces include vertical shear and moment. Vertical shear is checked at two critical locations, one at the beam end and another at the first opening. The beam end has the largest shear force. The shear force at the first opening is near the largest value but the strength is reduced due to the web opening.

Unlike W-beams which are checked for moment capacity based on their section modulus, the flexural capacity for castellated beams is based on the axial strength of the tee section similar to a Vierendeel truss. As moment is a force couple of compression and tension over a distance, these forces act on the tee sections. For a given section that has equal magnitudes of compression and tension, compression is checked because buckling strength governs over yielding strength. Each of these limit states have been worked out for a design case as shown in the first example.

Castellated beams can also be designed efficiently as composite members. Many limit state design checks are similar to non-composite castellated beams, but there are some differences. With the concrete slab carrying most if not all of the compression force, an asymmetric section can be utilized. By reducing the compression force that the top tee section experiences, the top base beam can be several sizes smaller than the bottom base beam whose tee experiences tension. In addition, the concrete slab carries some of the global shear force, reducing the shear forces in the tees thus Vierendeel bending moments. A composite design example was also worked out with these changes and is shown in the second example.

With so many variables in designing castellated beams, checking each limit state by hand can be lengthy. By inputting a beam and the cutting pattern into a spreadsheet or computer program the limit states can be determined and checked against global forces for design cases. Using design programs, structural engineers can easily compare several beam sizes and different cutting patterns to determine the most efficient design. These different patterns can include web post length variance along the length of the beam, so each tee and web post has a different design capacity. It is also possible to design castellated beams from cambered W-beams, either for architectural purposes or to meet serviceability requirements. Variability in design of castellated beams provides flexibility in architectural design, and stronger floors in buildings.

# References

American Institute of Steel Construction. (2017). *Steel Construction Manual* (15th Edition). AISC.

American Institute of Steel Construction. (2016). *Steel Design Guide 31 Castellated and Cellular Beam Design*. AISC.

American Society of Civil Engineers. (2017). *Minimum Design Loads and Associated Criteria for Buildings and Other Structures*. ASCE.

Grünbauer, Johann. *What are Castellated Beams?* Grünbauer BV.

http://www.grunbauer.nl/eng/wat.htm

Grünbauer, Johann. *Traditional Patterns*. Grünbauer BV.

http://www.grunbauer.nl/eng/raatvorm.htm

Marmors Group. (2021). *Castellated Beams*. Marmors Group.

http://www.marmorsgroup.com/steel-structures/castellated-beams

Precast/Prestressed Concrete Institute. (2017). *Design Handbook Precast and Prestressed Concrete*. PCI.

Tsavdaridis, K. & D'Mello, C. (2012). Vierendeel Bending Study of Perforated Steel Beams with Various Novel Shapes of Web Openings. *Journal of Structural Engineering, 138*(10), 1214-123. https://ascelibrary.org/doi/10.1061/%28ASCE%29ST.1943-541X.0000562

Vulcraft. (2008). *Steel Roof & Floor Deck*. Steel Deck Institute.